

# Lignin Pyrolysis Components and Upgrading—Technology Review

Wei Mu · Haoxi Ben · Art Ragauskas · Yulin Deng

Published online: 27 February 2013  
© Springer Science+Business Media New York 2013

**Abstract** Biomass pyrolysis oil has been reported as a potential renewable biofuel precursor. Although several review articles focusing on lignocellulose pyrolysis can be found, the one that particularly focus on lignin pyrolysis is still not available in literature. Lignin is the second most abundant biomass component and the primary renewable aromatic resource in nature. The pyrolysis chemistry and mechanism of lignin are significantly different from pyrolysis of cellulose or entire biomass. Therefore, different from other review articles in the field, this review particularly focuses on the recent developments in lignin pyrolysis chemistry, mechanism, catalysts, and the upgrading of the bio-oil from lignin pyrolysis. Although bio-oil production from pyrolysis of biomass has been proven on commercial scale and is a very promising option for production of renewable chemicals and fuels, there are still several drawbacks that have not been solved. The components of biomass pyrolysis oils are very complicated and related to the properties of bio-oil. In this review article, the details about pyrolysis oil components particularly those from lignin pyrolysis processes will be discussed first. Due to the poor physical and chemical property, the lignin pyrolysis oil has to be upgraded before usage. The most common method of upgrading bio-oil is hydrotreating. Catalysts have been widely used in petroleum industry for pyrolysis bio-oil upgrading. In this review paper, the mechanism of the hydrodeoxygenation reaction between the model compounds and catalysts will be discussed and the effects of the reaction condition will be summarized.

**Keywords** Lignin · Pyrolysis · Catalyst · Oil upgrade · Hydrodeoxygenation · Biofuel

## Introduction

The US Department of Agriculture and US Department of Energy established a vision to derive 25 % of chemicals and materials and 20 % of transportation fuels from biomass by 2030 [1]. Domestic energy consumption is continuing to expand and further resources will need to be tapped in the future to accommodate growth and expansion while reducing the exploitation of dead dinosaur fuel. There are many highlights in the United States alone for the consumption of energy including [2, 3]:

- Domestic energy consumption has increased by 28 % since 1973 from 75 to 97 quadrillion Btu of energy with a large percentage (28 % in 2010) of energy used for the transportation sector.
- Annual energy consumption from renewable resources is on pace to double from the year 2001 to 2012.
- Renewable energies now contribute more energy to domestic consumption than that of nuclear electric power.
- Annual consumption of fuel ethanol has more than tripled between 2005 and 2011 while biodiesel is on pace to more than double in 2012 over the previous year.

The remarkable growth in renewable transportation fuels in the USA is being realized due to changes in economic and political policies as well as changing consumer demand. Politicians are quick to throw out buzz phrases and tout national security concerns for the impetus to increase alternative fuels production, even though we import 33 % less petroleum from OPEC countries than non-OPEC countries [2]. Environmentalists and scientists make the argument to reduce carbon emissions which have been shown to contribute to global warming and cause changes to farming practices [4–9].

---

W. Mu · Y. Deng  
School of Chemical and Biomolecular Engineering, Georgia Institute of Technology, 500 10th Street NW, Atlanta, GA 30332, USA

W. Mu · H. Ben · A. Ragauskas · Y. Deng (✉)  
Institute of Paper Science and Technology, Georgia Institute of Technology, 500 10th Street NW, Atlanta, GA 30332, USA  
e-mail: yulin.deng@ipst.gatech.edu

H. Ben · A. Ragauskas  
School of Chemistry and Biochemistry, Georgia Institute of Technology, 500 10th Street NW, Atlanta, GA 30332, USA

There is a vast potential supply of sustainable renewable biomass from forest and agricultural lands throughout the world. The United States alone has the ability to provide more than 1.3 billion dry tons annually to supply bio-refineries [10]. Therefore, it is imperative that efforts are contributed towards advancing the science of converting renewable materials such as trees into other useful products such as fuels, specialty chemicals, and plastics. Parikka claimed the sustainable global biomass energy potential is  $\sim 10^{20}$  J per year ( $\sim 9.478 \times 10^{16}$  Btu per year) and  $\sim 40\%$  was being used [11]. It is also imperative that all fractions of the tree be used for the highest value products obtainable for that specific fraction. There has been a great deal of research with turning cellulose and hemicellulose into ethanol, while lignin has been utilized predominately as an agricultural waste for the production of steam to run the process. However, lignins' unique structure is well suited for specialty chemicals and high-value fuels.

Biomass represents a renewable and carbon-neutral resource for the production of bio-fuels and bio-chemicals. Generally, biomasses contain around 35–50 % of cellulose which is a polymer of  $\beta$ -(1,4)-glucan with a degree of polymerization of  $\sim 300$ –15,000, 25–30 % of hemicellulose which is a short-chain branched and substituted polymer of sugars with a degree of polymerization of  $\sim 70$ –200 and another 15–30 % of lignin which is a polymer derived from coniferyl, coumaryl, and sinapyl alcohol [12]. Pyrolysis is a thermochemical conversion process which could break down the biomass using heat in the absence of oxygen [13]. The products are in gas, liquid, and solid form. The solid form products are mainly recognized as char with high energy [14]. However, it is not a preferred as the liquid product. The liquid product of pyrolysis of biomass—pyrolysis oils are dark brown liquids which are comprised of hundreds of highly oxygenated organic compounds [14].

As the second most abundant biomass component and the primary renewable aromatic resource in nature, lignin, however, has received much less attention than plant polysaccharides as a resource for biofuels. Among the various conversion technologies being investigated, pyrolysis has been reported as one of the economic ways (i.e., low capital and operating costs) to utilize biomass for bio-fuels and bio-chemicals [15]. The pyrolysis of lignin yielding low-molecular weight compounds has been examined for the past 50 years. The lignin pyrolysis products are complicated. To fully understand the lignin pyrolysis process and develop more effective pyrolysis technology, new analysis methods for characterization of the lignin pyrolysis products have been developed recently. This review will summarize the new developments in lignin pyrolysis, including the new methods for analyzing the lignin pyrolysis products, the composition of lignin pyrolysis oil, upgrading the oil and mechanism study of lignin pyrolysis oil upgrading using model compounds.

## Gas Products of Pyrolysis of Lignin

From the 1980s to the early 2000s, many lignin pyrolysis researches focused on the gas products [16–22]. Some major gas components reported in the literature have been summarized in Table 1. Carbon monoxide and carbon dioxides are the top two most abundant components in the gas phase of pyrolysis of lignin. Normally, more than half percentages of gas products are these two components [16–21]. Methane has also been reported as another major gas component and the yield could be up to  $\sim 5$  wt.% of dry lignin [16, 17]. Methane, carbon monoxide, and carbon dioxides were found to increase in yield as the reactor temperature increased from 773 to 1,173 K [17, 18, 21, 22]. Nevertheless, the content of methane decrease at a higher heating rate [19]. Most interestingly, Ferdous et al. [19, 20] indicated that pyrolysis of lignin also produce  $\sim 25$  mol% of  $H_2$  in the gas phase and the content significantly increased with increasing thermal conversion temperature. It is well known that  $H_2$  and CO are the major components of syngas which could be used to produce synthetic petroleum, whereas the gas products of pyrolysis of lignin could also be used as syngas. The possible major gas production pathways are summarized in Fig. 1.

## Solid Products of Pyrolysis of Lignin

In the literature there are considerable works have been done on the characterization of volatile products (including gas and tar) produced from pyrolysis of lignin; however, there is very limited information on the other important product—char. It has been reported that char has a condensed aromatic structure and reserve up to 50 % of energy from starting biomass [23]. Sharma et al. [24, 25] has done very detailed characterization of lignin char by SEM, FTIR, and CPMAS  $^{13}C$  NMR. The char yield decreased from  $\sim 80$  to  $\sim 40$  wt.% of lignin as the pyrolysis temperature increased from 523 to 1,023 K. The authors also indicated that based on FTIR and NMR results the cleavages of aliphatic OH, carboxyl, and methoxyl groups have been improved at higher pyrolysis temperature. As a result, both H/C and O/C ratios decreased at a higher thermal treatment temperature, which represents a condensed aromatic structure. Hosoya et al. [26] have investigated the influence of methoxyl group in char formation from lignin model compounds by GC-MS analysis. They indicated that methoxyl groups are one of the necessary requirements for the char formation during lignin pyrolysis process. In addition, *o*-quinone methide was found to be an important intermediate during lignin char formation process. Chu et al. [27] examined the pyrolytic behavior of a  $\beta$ -O-4 type lignin model polymer at 523–823 K and characterized the products by TGA, FTIR, GPC, GC-MS,  $^1H$ ,

**Table 1** Reported major gas products of pyrolysis of lignin

Major gas components of pyrolysis of lignin <sup>a</sup>				
CH <sub>4</sub> [16–22]	C <sub>2</sub> H <sub>4</sub> [16–18, 21, 22]	C <sub>2</sub> H <sub>6</sub> [16–18, 21, 22]	C <sub>3</sub> H <sub>6</sub> [16–18, 21, 22]	C <sub>4</sub> H <sub>8</sub> [16–18, 21, 22]
CO [16–22]	CO <sub>2</sub> [16–21]	H <sub>2</sub> [19, 20]	HCHO [16, 18, 22]	CH <sub>3</sub> CHO [16–18, 22]

<sup>a</sup> The pyrolysis temperatures are from 573–1,273 K and lignins are isolated from both softwood and hardwood by kraft and ethanol-based pulping process

and <sup>13</sup>C NMR. The authors proposed some possible reaction mechanisms of pyrolysis of lignin model polymer and indicated that the formation of char was due to polymerization of small radical species and the elimination of side functional groups including hydroxyl and methoxyl groups will terminate the polymerization and finally form the char. The possible char formation pathways are summarized in Fig. 1.

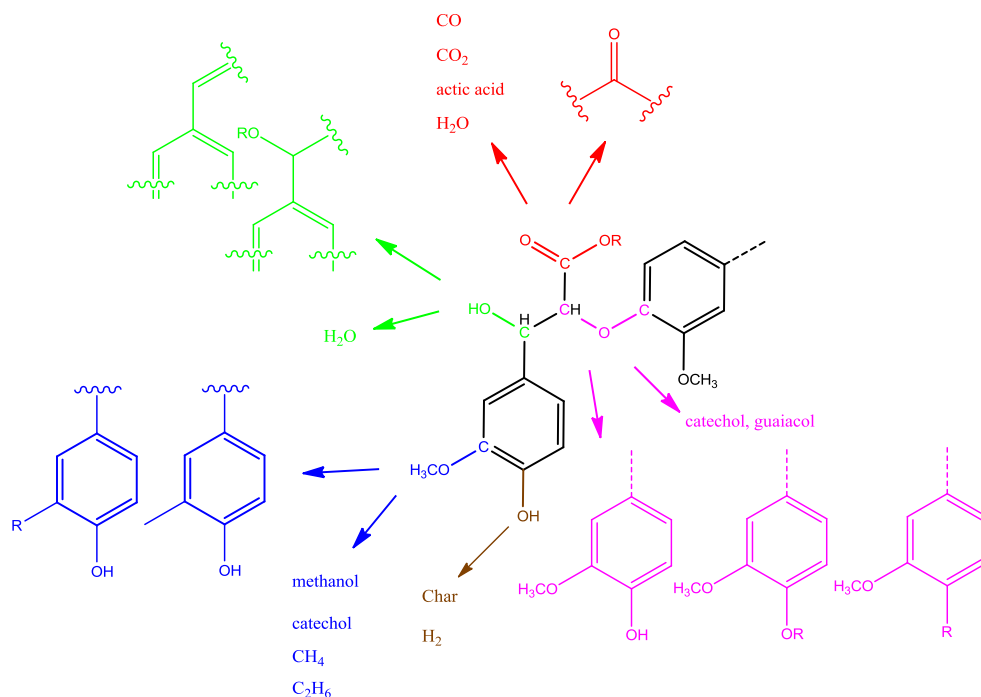
### Liquid Products of Pyrolysis of Lignin

#### GC-MS Analysis of Lignin Pyrolysis Oil

Most of pyrolysis works employed GC-MS to analyze the liquid pyrolysis products [28–44]. By using pyrolysis(Py)-GC-MS, Jimenez et al. [44] indicated that softwood lignins yielded guaiacyl derivatives, coniferaldehyde, and coniferyl alcohol as the major products; hardwood lignins gave guaiacyl and syringyl derivatives, syringaldehyde, coniferyl alcohol, and sinapyl alcohol. Pyrolysis of bamboo lignin produced p-vinylphenol as the major compound. Similarly, Jiang et al. [32] also used Py-GC-MS to analyze pyrolysis products of

lignin over a temperature range of 673–1,073 K and indicated that the maximum yield of phenolic compounds was obtained at 873 K. Most of the phenolic compounds had an individual yield of less than 1 wt.% of lignin on a dry-ash-free basis. Greenwood et al. [39] pyrolyzed *Douglas* fir and *Quercus nigra* water oak lignin in a laser micropyrolysis-GC-MS system. They found that guaiacol, 4-methyl-guaiacol, vinylguaiacol, eugenol, vanillin, and coniferylaldehyde are the major components in the pyrolysis oil produced from *Douglas* fir lignin. For the *Q. nigra* water oak lignin pyrolysis oil, guaiacol, 4-methyl-guaiacol, vinylguaiacol, syringol, eugenol, 3,5-dimethoxyacetophenone, 4-methyl 2,5-dimethoxy benzaldehyde, 4-allyl-dimethoxyphenol, syringaldehyde, 2,6-dimethoxyl-2-propylphenol, and sinapaldehyde are found as the major components. Jegers et al. [41] also indicated that guaiacol, 4-methylguaiacol, 4-ethylguaiacol, catechol, 4-methylcatechol, 4-ethylcatechol, phenol, cresol, and 4-ethylphenol are the major products of pyrolysis of lignin. As the most abundant products, the content of guaiacol and 4-methylguaiacol are ~5.3 wt.% of dry lignin. Lou et al. [34] examined the effect of temperature on the composition of pyrolysis products and indicated that the contents of methoxyl

**Fig. 1** The possible decomposition pathways of lignin during the pyrolysis [27, 140–146]



contained components such as guaiacol, 4-methylguaiacol, 4-vinylguaiacol, and syringol decreased at higher pyrolysis temperature. In contrast, the contents of non-methoxyl contained compounds, like cresols, ethyl-phenol, and 2, 6-dimethyl-phenol increased with increasing treatment temperature.

To understand the possible decomposition pathways of lignin during the pyrolysis process and to find an effective upgrading method, many researchers choose to use pyrolysis oil model compounds to simplify the simulation model. To facilitate this part of work, in Table 2, we summarized the GC-MS detected components in the lignin pyrolysis oils reported from seven literatures [32, 38–43]. There are approximately a hundred compounds in Table 2 and almost all of them contain a phenol structure. Furthermore, phenol, acetovanillone, cresols, guaiacol, 4-ethylphenol, syringaldehyde, acetosyringone, 4-methylguaiacol, catechol, 3-methylcatechol, 4-methylguaiacol, 4-vinylguaiacol, vanillin, syringol, eugenol, isoeugenol, and acetovanillone have been reported in more than four references and many of them also could be found in other references [30, 33–35, 37]. Therefore, these components could be used as potential candidates for the model compounds study about pyrolysis of lignin. A summary of lignin pyrolysis conditions and the yield of pyrolysis products are shown in Table 3. The possible decomposition pathways are shown in Fig. 1.

#### FTIR Analysis of Lignin Pyrolysis Oil

Most compounds in the Table 2 have a molecular weight below 220 g/mol. However, some researchers have detected the average molecular weight of lignin pyrolysis oil by GPC and reported that the molecular weights are from 210 to 1,300 g/mol [45–47]. Due to the limitation of volatility of high molecular weight components in the pyrolysis oil, it has been indicated that there are only about 40 % of pyrolysis oil that could be detected by GC [14]. Therefore, many researchers also try to find alternative characterization method which could analyze the whole portion of pyrolysis oil, such as FTIR [43, 48–53]. Liu et al. [50] did a mechanistic study of hardwood and softwood lignin pyrolysis using a thermogravimetric analyzer coupled with a Fourier transform infrared spectrometry (TG-FTIR). They indicated that lignin undergoes three consecutive sets of reactions during pyrolysis including the evaporation of water, the formation of primary volatiles and the release of small molecular gases. At first, the absorbed water is released by evaporation, and then at a higher temperature (above 373 K) water is generated by the dehydration of lignin aliphatic hydroxyl groups. The authors also indicated that phenols, in addition to alcohols, aldehydes, acids, and CO, CO<sub>2</sub> CH<sub>4</sub> were the major gaseous products. Scholze et al. [43] also characterized pyrolysis oil by FTIR and indicated a correlation

between carbonyl absorption bands and oxygen content as well as carbon content. To facilitate this promising fast analysis method of pyrolysis oils, we summarized the assignment ranges from six references and shown this result in Table 3.

#### NMR Analysis of Lignin Pyrolysis Oil

It is well known that pyrolysis oil is a very complex mixture, whereas the ability of FTIR for comprehending the details of pyrolysis oil is limited. Most recently, some research work [46, 47, 54–63] introduce NMR, including quantitative <sup>1</sup>H, <sup>31</sup>P, and <sup>13</sup>C-NMR, and semi-quantitative HSQC-NMR to characterize pyrolysis oils. Mullen et al. [54] analyzed various pyrolysis oils produced from switchgrass, alfalfa stems, corn stover, guayule (whole plant and latex-extracted bagasse), and chicken litter by <sup>1</sup>H, <sup>13</sup>C, and <sup>13</sup>C-DEPT (distortionless enhancement polarization transfer)-NMR. They found that pyrolysis oil from chicken litter had the lowest overall amount of methyl groups and had the highest ketone content of the pyrolysis oils studied. The <sup>13</sup>C and DEPT-NMR analysis indicated that the pyrolysis oils from corn stover and switchgrass had the fewest aliphatic carbons. The large amount of methine (CH<sub>1</sub>) groups in the corn stover pyrolysis oil suggested that its aliphatics were highly branched. However, there were almost the same amounts of methyl (–CH<sub>3</sub>) groups as its methine groups, while the percentage of –CH<sub>2</sub>– was low, it was surmised that these branches were very short which could mostly be methyl groups. Conversely, pyrolysis oil from switchgrass appeared to have more straight-chain aliphatics. The authors also indicated that the aromatic region of these pyrolysis oils had CH<sub>0</sub>:CH<sub>1</sub> ratios of >2:1, which represents highly complex substituted (at least four substituents) benzene rings.

Our previous work [47] used <sup>31</sup>P and <sup>13</sup>C-NMR to characterize pyrolysis oils produced from softwood (SW) kraft lignin at 673, 773, 873, and 973 K. A <sup>13</sup>C-NMR database was created to provide a more accurate chemical shift assignment for analysis of pyrolysis oils. This analysis showed that the carbonyl group content was reduced after pyrolysis, and methoxyl group was significantly eliminated after pyrolysis, especially at higher pyrolysis temperatures. Nearly 70–80 % of the carbons from water-insoluble portion of pyrolysis oil (heavy oil) are aromatic carbon. By using <sup>31</sup>P-NMR, the results indicated that the heavy oils contained less aliphatic hydroxyl group and carboxyl acid group. The decreased concentration of aliphatic hydroxyl and acid groups was significant as it indicated that the lignin side chain hydroxyl groups were readily eliminated during the thermal treatment. In contrast, the content of guaiacyl, p-hydroxyphenyl and catechol type hydroxyl groups increased after pyrolysis. The <sup>31</sup>P-NMR results for the water soluble part of pyrolysis oil (light oil) showed that it contained

**Table 2** Reported liquid products of pyrolysis of ligninGC-MS detected components in lignin pyrolysis oil<sup>a</sup>

Phenol [32, 38–43]	4'-Hydroxy-3'-methoxyacetophenone [32, 38–40, 42, 43] Acetovanillone Acetoguaiacone	4-Allyl-dimethoxyphenol [39]
2-Methylphenol [32, 38–43] o-Cresol	5-Tert-butylpyrogallol [32]	Dimethoxypropylphenol [39]
4-Methylphenol [32, 38, 39, 41, 42] p-Cresol	1-(4-Hydroxy-3-methoxyphenyl)-2-propanone [32, 42, 43] Guaiacylacetone	Coniferylaldehyde [39, 43]
2-Methoxyphenol [32, 38–43] Guaiacol	2-(3,4-Dimethoxyphenyl)-6-methyl-3,4-chromanediol [32]	Sinapaldehyde [39, 43]
2,6-Dimethylphenol [32, 40, 42] 2,6-Xylenol	3,4-Dimethylbenzoic acid [32, 40]	2,6-Dimethoxy-4-methylphenol [38, 43] 4-Methylsyringol
4-Ethylphenol [32, 38, 41, 42] p-Ethylphenol	3-Methoxy-4-hydroxybenzoic acid [32]	1-(4-Hydroxy-3-methoxyphenyl) propyne [38]
3-Methylbenzaldehyde [32] m-Tolualdehyde	4-Ethyl-1,2-dimethoxybenzene [32]	4-Ethyl-2,6-dimethoxyphenol [38, 43] 4-Ethylsyringol
2-Hydroxy-6-methylbenzaldehyde [32]	4-Propenylsyringol [32, 38, 43] 4-Propenyl-2,6-dimethoxyphenol	4-Vinyl-2,6-dimethoxyphenol [38, 43] Vinylsyringol
2-Ethylphenol [32, 41, 42]	Ferulic acid [32] 3-Hydroxy-4-methoxycinnamic acid	4-Propyl-2,6-dimethoxyphenol [38]
4-Methoxy-3-methylphenol [32]	4-Hydroxy-3,5-dimethoxybenzaldehyde [32, 38, 39, 42, 43] Syringaldehyde	Syringylacetone [38, 43]
2-Methoxy-4-methylphenol [32, 38–43] 4-Methylguaiaacol	Acetosyringone [32, 38, 39, 42] 4'-Hydroxy-3',5'-dimethoxyacetophenone	m-Cresol [40, 41]
Catechol [32, 39–42] 1,2-Benzenediol	1-(2,6-Dihydroxy-4-methoxyphenyl)-1-butanone [32] Desaspidinol	p-Propylphenol [41]
Benzofuran [32]	Syringic acid [32] 4-Hydroxy-3,5-dimethoxybenzoic acid	6-Ethylguaiaacol [41]
p-Isopropylphenol [32] p-Cumenol	2,3,5-Trimethyl phenol [42]	2-Methoxy-4-propylphenol [40, 41, 43] 4-Propylguaiaacol
2-Ethyl-4-methylphenol [32]	3-Ethyl phenol [40–42]	4-Methyl-1,2-benzenediol [40, 41] 4-Methylcatechol
3-Methoxy-1,2-benzenediol [32, 41, 42] 3-Methoxycatechol	1,2,3-Trimethoxybenzene [42]	6-Ethylcatechol [41]
3-Methyl-1,2-benzenediol [32, 39–42] 3-Methylpyrocatechol 3-Methylcatechol	Coniferyl alcohol [40–42]	3-Methylguaiaacol [43]
2-Methoxy-4-ethylphenol [32, 38–43]	Methoxyeugenol [38, 42] 4-Hydroxy-3,5-dimethoxyallylbenzene 4-Allyl-2,6-dimethoxyphenol	3-Ethylguaiaacol [43]
4-(2-Propenyl)phenol [32]	1-Methoxy-3-methylbenzene [39]	Propioguiacone [43] 1-(4-Hydroxy-3-methoxy-phenyl)-propan-1-one
p-Isopropenylphenol [32]	Indene [39]	6-Hydroxy-5,7-dimethoxy-indene [43]
2-Methoxy-4-vinylphenol [32, 38, 39, 42, 43] 4-Vinylguaiaacol	1,2,3-Trimethylbenzene [39]	Dihydroconiferylalcohol [43]
3-Methyl-5-methoxyphenol [32]	1,2,4-Trimethylbenzene [39]	Propiosyringone [43]
4-Ethyl-1,3-benzenediol [40] 4-Ethylresorcinol	Mesitylene [39]	Dihydrosinapylalcohol [43]
2,6-Dimethoxyphenol [32, 38, 39, 42, 43] Syringol	4-Ethenylphenol [38, 39] Vinylphenol	Sinapylalcohol [43]
2,5-Dimethyl-1,4-benzenediol [32]	m-Dimethoxybenzene [39]	2,3-dimethylphenol [40] 2,3-xylenol
2,4-Dimethoxyphenol [32]	Veratrole [39]	Naphthalene [39, 40]
2',4'-Dimethylacetophenone [32]	p-Dimethoxybenzene [39]	Benzene [42]
4-Ethyl-1,2-benzenediol [32, 41] 4-Ethylpyrocatechol	Dimethylcatechol [39]	Styrene [42]
Eugenol [32, 38–40, 42, 43]	Vinylcatechol [39]	p-Xylene [42]
3-Hydroxy-4-methoxybenzaldehyde [32, 39, 42] Isovanillin	Vanillin [38–40, 43]	Ethylbenzene [42]
2,5-Dimethoxybenzylalcohol [32]	3',5'-Dimethoxyacetophenone [39]	Toluene [42]

**Table 2** (continued)GC-MS detected components in lignin pyrolysis oil<sup>a</sup>

2-Methoxy-4-(1-propenyl)phenol [32, 38–40, 42, 43] Isoeugenol	4-Methyl 2,5-dimethoxy benzaldehyde [39]
4'-Hydroxy-3'-methoxyacetophenone [32, 38–40, 42, 43] Acetovanillone	Fluorene [39]

<sup>a</sup> The pyrolysis temperatures are from 673 to 1,073 K

nearly 80 % w/w water and another 10 % w/w was methanol, catechol, and acetic acid.

To solve spectral overlapping problems when using <sup>13</sup>C-NMR to analyze the pyrolysis oils, our previous work [62] demonstrated that HSQC-NMR was uniquely well suited to analyze various C-H bonds present in the pyrolysis oils. The fingerprint analysis of HSQC-NMR spectral data provided chemical shift assignment of 27 (14 from lignin pyrolysis oil) different types of C-H bonds present in pyrolysis oils produced from cellulose, lignin, and pine wood. The HSQC-NMR for the lignin pyrolysis oils showed that there were two different types of methoxyl group present in the pyrolysis oils, which indicated that the native methoxyl group in the kraft lignin will rearrange to another type during the thermal treatment. The content of aromatic C-H and aliphatic C-H bonds in the lignin pyrolysis oils increased with increasing pyrolysis temperature, which was attributed to the rearrangement and the cleavage of ether bonds or methoxyl groups in the lignin structure. Table 4 summarized the functional groups present in lignin pyrolysis oils could be analyzed by NMR (Table 5).

## Introduction to Bio-oil Upgrading

The major products in lignin-derived pyrolysis oil are discussed and listed in [Gas products of pyrolysis of lignin](#) and [Solid products of pyrolysis of lignin](#) sections. However, the produced oil cannot be used directly as fuel due to several poor properties, such as thermal instability, corrosiveness, poor volatility, high coking tendency, low heating value, and immiscible with petroleum fuels [66]. The two key differences between bio-oil from pyrolysis and traditional oil are the high oxygen content and high unsaturated content. Therefore, upgrading is a necessary step of the lignin-derived pyrolysis oil to meet the fuel specification.

The catalytic bio-oil upgrading involves a series of complex reactions. Generally speaking, the upgrading process stabilizes the bio-oil, reduces or eliminates the poor properties mentioned above and makes it compatible with gasoline. The most common upgrading routes are hydrodeoxygenation (HDO) and zeolite cracking. Mortensen et al. gave a detailed review on the whole biomass derived bio-oil upgrading by using HDO and zeolite method [65]. Huber and Corma et al.

**Table 3** Summary of lignin pyrolysis conditions and the yield of pyrolysis products

Lignin	Reactor	Temperature (K)	Tar (wt.%)	Char (wt.%)	Gas (wt.%)
Kraft lignin (wheat straw and sarkanda grass) [42]	Fluidized bed	773	31	49	6
	Fluidized bed	683–833	31	34	12
	Fluidized bed	748–798	50	42	8
	Entrained flow	973	37	35	28
	Batch	753	22	48	30
Kraft lignin (pine)	Fluidized bed [147]	823	23	41	39
Lignoboost <sup>TM</sup> (pine)			22	29	49
EOL ( <i>pinus radiata</i> )			16	63	21
Kraft lignin	Fixed bed [19]	1,073	3–5	43–48	49–52
			EOL	14–21	35–44
Kraft lignin	Fix bed [20]	923	13	47	40
			EOL	19	39
Klason lignin (almond shells) [18]	Micro pyroprobe reactor	773	53	34	7
		873	64	20	9
		973	55	17	17
		1,073	50	15	22
		1,173	43	14	29

**Table 4** FTIR assignments of lignin pyrolysis oil

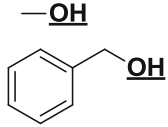
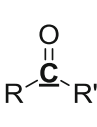
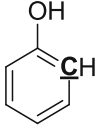
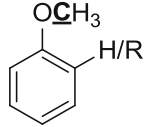
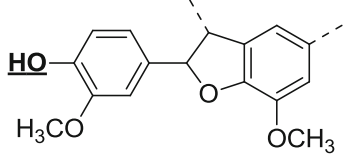
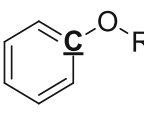
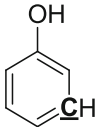
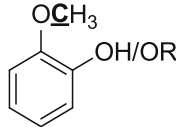
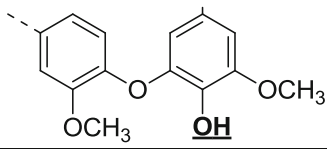
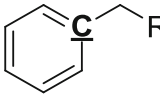
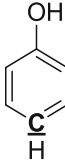
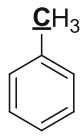
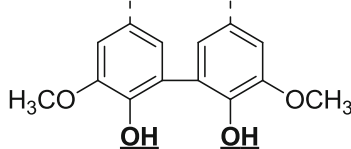
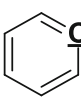
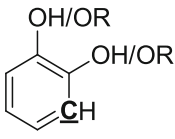
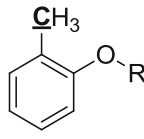
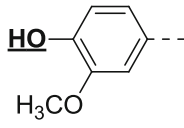
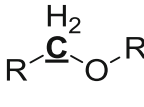
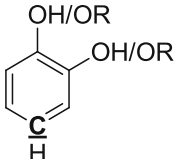
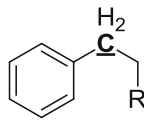
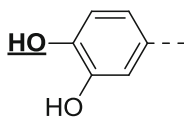
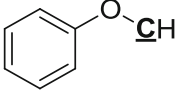
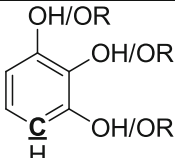
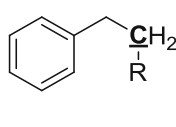
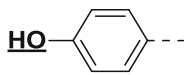
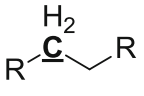
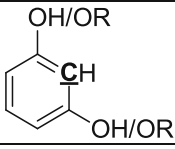
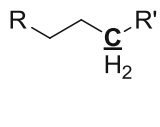
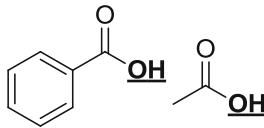
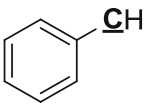
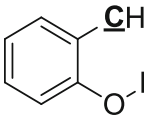
Wave number (cm <sup>-1</sup> )	Assignments [43, 48–50, 52, 53]
3429	O-H stretching vibration, H <sub>2</sub> O
1701–1734	C=O stretch in unconjugated ketones, carbonyl and ester groups
1652–1666	C=O stretch in conjugated aryl ketones
1593–1609	Aromatic ring vibrations and C=O stretch
1504–1515	Aromatic ring vibrations
1462–1464	Asymmetric C-H bending (in CH <sub>3</sub> and –CH <sub>2</sub> –)
1420–1424	Aromatic ring vibrations
1365	Symmetric deformation of C-H in methyl groups
1360	Phenolic hydroxyl vibrations
1270	Vibrations of guaiacyl rings and stretching vibrations of C-O bonds
1214–1233	C-C, C-O, and C=O stretching
1190	Vibrations of methoxyl group
1160	Deformation vibrations of C-H bonds in benzene rings
1140	Deformation vibration of C-H bonds in guaiacyl rings
1115	Vibrations of ester linkage
1114–1125	Aromatic in-plane C-H bending
1075–1090	Deformation vibrations of C-O bonds in secondary alcohols and aliphatic ethers
1030–1033	Deformation vibrations of C-H bonds in aromatic rings
914–919	Aromatic out-of-plane C-H bending
852–859	Aromatic out-of-plane C-H bending in positions 2, 5, and 6 of guaiacyl units
833	Vibrations of C-H bonds in syringyl units

also reviewed the synthesis of transportation fuel from whole biomass and both upgrading methods were introduced in the bio-oil upgrading section [66]. Briefly speaking, HDO process produces high-quality oil, but it requires hydrogen under pressure as reactant. The cost for hydrogen and pressurized reactor is a big barrier for the promotion of HDO process. Zeolite cracking only requires low amount hydrogen and regular non-pressurized reactor. However, the produced oil is in low quality (low H/C ratio) [67] and the coking problem is much stronger than it is in the HDO process [68]. Moreover, although zeolite is effective in deoxygenation with small oxygenates (such as aldehydes and ketones), their capability for phenolics deoxygenation is limited because of the small pore opening [69–71]. This paper will only discuss the catalysts used in HDO and related reaction mechanism.

Hydrodeoxygenation, as the name indicated, contains hydrogenation and deoxygenation parts. The common features of key model compounds for pyrolysis oil are oxygen atoms and aromatic structure. The purpose for HDO is to hydrogenate the unstable unsaturated bonds and reduce the oxygen in the pyrolysis oil. Research showed that the pyrolysis oil tends to repolymerize under 448–523 K without catalyst or hydrogen, followed by char formation within a couple of minutes [72]. However, in the presence of catalyst and hydrogen, the pyrolysis oil will convert to stable compounds first under the same condition. When the temperature goes higher than 523 K, the HDO reaction occurs with the existence of hydrogen and catalyst.

In 1983, Furimsky et al. published the first review paper on the catalyst, mechanism, and kinetics study related to HDO process in crude oil upgrading [73]. Very limited information was available at that time. Afterwards, numerous papers appeared in HDO study on coal-derived liquid and biomass-derived oil. In 2000, Furimsky et al. reviewed the catalytic hydrodeoxygenation again [74]. This time much more detailed information was included that the phenol, furan, ether, and other bio-oil compounds were all included. Huber and Corma et al. reviewed the synthesis of transportation fuel from biomass [66]. However, both of the two reviews focused on the model compounds related to whole biomass-derived oil. Elliott discussed the hydroprocessing of bio-oil from whole biomass in his review paper published in 2007 [75]. It focused on the HDO of bio-oils made from various liquefaction methods. In 2011, Choudhary reviewed the HDO process related to two bio-related feed stocks, (a) high content of triglycerides oil and (b) high-pressure liquefaction-derived oil and pyrolysis-derived oil [76]. Mortensen et al. discussed the two major upgrading routes, HDO and zeolite upgrading on whole biomass-derived oil [65]. In 2012, Bu et al. reviewed the catalytic hydrodeoxygenation of lignin-derived phenols [77]. Phenol compound HDO was discussed intensively in the paper. Most of the review paper mentioned above only related to the bio-oil from whole biomass. This review paper focuses on the catalyst behaviors and reaction mechanism study of lignin-derived bio-oil

**Table 5** NMR detectable functional groups in lignin pyrolysis oils [46, 47, 54–63]

$^1\text{H-NMR}$ [46, 54, 55, 58, 63]	$^{31}\text{P-NMR}$ [47, 57, 59-61]	$^{13}\text{C-NMR}$ [54, 56-61, 63]	HSQC[62]	
$-\underline{\text{CHO}}$ , $-\underline{\text{COOH}}$				
$\text{Ar}\underline{\text{H}}$ , $\underline{\text{HC}}=\text{C}-$				
$-\underline{\text{CH}}_n\text{-O-}$ , $\underline{\text{CH}}_n\text{-O-}$				
$-\underline{\text{CH}}_3$ , $-\underline{\text{CH}}_n-$				
				
				
				
				
				

HDO process. Only heterogeneous catalysts will be introduced because the separation of homogeneous catalysts from the reaction solution is still a big problem in the application.

### Source of Hydrogen and Economic Analysis

Hydrogen plays a key role in the upgrading of pyrolysis oil. In the report published by the International Energy Agency



[78], the author compared the process and cost of hydrogen generation from various methods such as electrolysis, natural gas reforming, coal gasification, thermal-water splitting, biomass, photo-electrolysis, and biological process. The result showed that natural gas reforming and coal gasification could produce hydrogen at lowest costs. The prices of hydrogen in unit GJ for natural gas reforming, coal gasification, and electrolysis were \$3–4, \$1–1.5, and \$35–55, respectively.

Besides using external sources, the hydrogen could also be produced from pyrolysis oil portion through aqueous phase reforming (APR). Pt/ $\gamma$ -Al<sub>2</sub>O<sub>3</sub> was reported in catalyzing APR reaction with low-boiling fraction of pyrolysis oil [79]. Although the hydrogen from APR was not enough for complete upgrading, it could partially reduce our dependence on the external source. Wright et al. analyzed the economic feasibility and concluded that this method could reduce the cost of bio-oil [80]. A more detailed study revealed that using portion of bio-oil would reduce the overall yield and potentially result in higher cost [81]. Therefore the amount of bio-oil for hydrogen production needs further optimization to minimize the cost. Another internal hydrogen source is the hydrogen generated in pyrolysis stage, which could also be collected and used in upgrading.

Several economic analyses have been done on bio-oil production through upgrading. In the study by Wright et al. [80], the author optimized the process and the minimum fuel selling price was 2.48 per gallon. The result is similar to another study done by PNNL [82]. Two years ago, another more relevant study on economic analysis was done on upgrading of fast pyrolysis oil [81]. Depending on various hydrogen sources, the cost of final oil product could be ranged from \$2.11 to 3.09. All these studies showed that bio-oil production through pyrolysis and upgrading is very competitive to traditional fossil fuel.

### Catalysts Used in Hydrodeoxygenation Process

Two types of catalysts are commonly used in HDO process. The first type is sulfide catalysts, such as NiMoS/Al<sub>2</sub>O<sub>3</sub>, CoMoS/Al<sub>2</sub>O<sub>3</sub>, etc. This type of catalyst is widely used in the petroleum industry for HDO purpose for decades [65, 74, 75]. The technique is mature and the reaction mechanisms are very well studied. The cost for this type of catalysts is much lower than the second type described below. Oxygen atoms in phenolic compounds can be effectively removed by these sulfided catalysts with high yields of aromatic and saturated products [74, 75, 83–86]. However, bio-oil is different to conventional fossil feedstock that the oxygen content in bio-oil is way higher than it is in the fossil oil and it is also inherently low amount of sulfur. Although these catalysts are good at oxygen removal, the

high amount of oxygen can cause rapid catalyst deactivation during the HDO [87]. Second, the water in raw bio-oil would also induce deactivation to the catalysts, therefore most of the reactions catalyzed by sulfide catalysts were conducted in gas phase [88]. The high coking formation would also reduce the life of the catalysts [88–90]. Some of the catalysts need sulfur during the reaction which would cause sulfur contamination [74].

The second type of catalysts is transition metal catalysts, including platinum, palladium, ruthenium, rhodium, etc. This type of catalyst is tolerant to the solvent that it can perform HDO reaction with the existence of water or even in water phase. Generally, noble metals have higher reactivity for hydrogenation and require less severe reaction condition than sulfided catalyst [92, 93]. One of the disadvantages of the experiment is that it is sensitive to sulfur. The feedstock with certain amount of sulfur requires special treatment to remove the sulfur before the HDO process. As long as the lignin is not produced by kraft pulping process, it is not a problem. Another problem is that the cost of this type of catalyst is very high so that the demanding catalyst recycle technique is also challenging.

### Sulfided Catalyst

The sulfided catalyst was firstly applied in HDO experiment in 1970 [94]. Lots of related research has been done since then. Weckhuysen gave a detailed review paper about the reaction conditions and catalysts [10]. In this paper, only the latest progress will be updated.

In the study by Ryymin et al. [95], the HDO of phenol over sulfided NiMo/ $\gamma$ -Al<sub>2</sub>O<sub>3</sub> was evaluated under 523 K and 7.5 MPa hydrogen. They found that the competition on active site greatly affected the selectivity, e.g., phenol was sensitive to the presence of the other reactant such as methyl heptanoate. The presence of sulfur-induced catalyst deactivation and decreased the fraction of cyclohexane, because the active sites for alkene saturation were occupied by sulfur. The sulfur-containing intermediates were also observed.

The temperature effect on guaiacol HDO was also evaluated by Lin et al. [96]. It was found that between 573 and 673 K, the yield of conversion was increased but the coke formation was decreased. The NiMo had high selectivity towards cyclohexane (~80 %) and CoMo produced more phenol and methyl-phenol. Cokes and sulfur stripping from catalyst were found on both NiMo and CoMo catalysts.

The conversion of monomeric and dimeric substrates on sulfide CoMo catalysts under 573 K and 5 MPa hydrogen revealed the extended reaction paths that HDO, demethylation, and hydrogenation happened simultaneously [97]. The forming of benzene from guaiacol had two paths: (1) methoxy removal first, then direct deoxygenation of phenolic -OH, (2) demethylation first, then remove both phenolic

–OH by HDO. Path 2 was the dominant pathway in the experiment since catechol was observed. In dimeric study, alkyl ether and  $\beta$ -O-4 bonds were broken. The 5-5' linkage left intact.

The promoter effect on MoS<sub>2</sub>-based catalyst was another key field in the application. Co and Ni are the two most common promoters for Mo-catalyst [98–100]. The reason for Ni/Co promoting effect was due to that the amount of active sites, mainly sulfur vacancies (coordinatively unsaturated sites), are higher than individual pure MoS<sub>2</sub> catalyst. Both promoters were able to donate electron to MoS<sub>2</sub>, which weakened the bonding between metal and sulfur and created more active sites [100]. Daudin et al. studied the Ni promoter effect and found that the Ni had dual role in the catalyst [98]. First, NiMoS mix phase promoted the HDO reaction. Second, Ni formed the Ni<sub>3</sub>S<sub>2</sub> (111) active site after sulfided. The HDO reaction was more favorable on the Ni<sub>3</sub>S<sub>2</sub> site than the MoS<sub>2</sub> site. Laurenti et al. [99] studied the Co promoter. The existence of Co formed CoMoS phase, which greatly enhanced the direct deoxygenation compared with MoS<sub>2</sub>. Richard et al. compared the Co and Ni promoter effect [100]. It was discovered that under 613 K and 7 MPa hydrogen, Ni had slightly higher activity than Co. Ni promoter favored hydrogenation with promoting factor of 3.4. Cobalt promoter favored direct deoxygenation reaction with promoting factor of 3.8. The difference was due to that the surface altered the preferred adsorption mode.

Travert et al. studied the water effect on Mo and CoMo catalysts in HDO [101]. The water would accelerate the deactivation of the catalyst because water occupied the active site (edge sulfur atoms). With only MoS<sub>2</sub>, it was only partially reversible. After adding the Co promoter, the water poisoning was lowered and it became fully reversible because Co atom could suppress the exchange between sulfur and oxygen.

## Noble Metal Catalyst

### Platinum

Platinum is the most extensively studied catalyst in this category. It is widely used in various HDO reactions and shows robust reactivity [64, 68, 91, 102–110]. The detailed reaction network for the model compounds are discussed in [Catalysts Used in Hydrodeoxygenation Process](#) section. In this section, we only focus on the catalyst behavior during the reaction.

Overall speaking, platinum is active in hydrogenation of the aromatic structure. To remove the oxygen in the compound, in most cases, the bifunctional catalyst is necessary because the removal of oxygen requires the acid site on the support material. Lobo et al. used Pt/ $\gamma$ -Al<sub>2</sub>O<sub>3</sub> as catalyst to hydrogenate meta-cresol under 533 K [102]. Platinum catalyst only hydrogenated the aromatic ring and the acid site on the

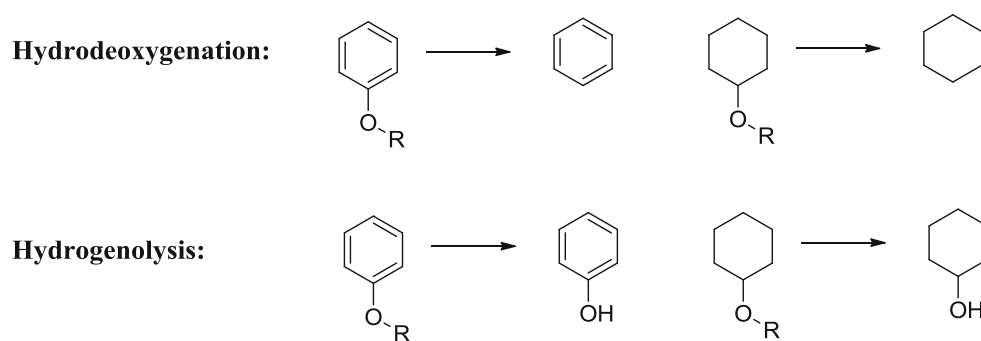
support promoted the dehydration reaction after the aromatic ring was hydrogenated. The kinetics study showed that phenolic ring saturation was the rate-limiting step. Increasing dispersion of platinum enhanced the hydrogenation activity [68]. The dispersion of platinum is not only determined by the surface area but also the surface chemistry of the support material. Jones et al. [103] found that platinum catalyst was efficient at ring saturation under 473 K. However, it did not remove the hydroxyl group on both phenol and cyclohexanol compounds. Bicyclic compounds were produced in the reaction, which indicated ring-coupling reaction occurred on the metal surface. Not only hydroxyl group, during the hydrogenation of guaiacol under 523 K, both methoxy and hydroxyl group were not removed by platinum alone [104].

However, another research showed that under some conditions, the oxygen could be partially or completely removed by platinum catalyst. Gates et al. [64] performed HDO experiments for four model compounds with Pt/ $\gamma$ -Al<sub>2</sub>O<sub>3</sub> catalyst under 573 K. Both HDO reaction and hydrogenolysis reaction were observed under the condition. The author defined the former as oxygen removal from the aromatic ring and the latter meant that oxygen still attached to the aromatic ring after the C-O cleavage (Fig. 2). The kinetics data was calculated for all four model compounds that hydrogenolysis reaction dominated in two of them (anisole, 4-methylanisole). For guaiacol, the hydrogenolysis reaction rate was still higher than the rate of HDO. After the aromatic ring was saturated, the Pt did not effectively deoxygenate the cyclohexanone and cyclohexanol under this condition.

Fukuoka et al. [107] used platinum supported on activated carbon (AC) to catalyze the 4-propyl-phenol HDO reaction in water phase at 553 K under acid-free condition. The aromatic structure was initially hydrogenated on the metal surface, and then the deoxygenated products were produced. In the NH<sub>3</sub>-TPD (temperature-programmed desorption) profile, Pt/AC showed no peak, which meant that there was no acidity site on the surface. Therefore, the acid-site catalyzed deoxygenation was not possible in the reaction. The hydrogenolysis reaction occurred on platinum surface. This catalyst was reused for three times and no deactivation was observed.

Besides hydrogenation and deoxygenation reactions, platinum is also able to catalyze the methyl removal/transfer reaction. Resasco et al. [105] did HDO experiment on anisole under 673 K with platinum on H $\beta$  zeolite as catalyst. Over the platinum metal, demethylation of anisole was the primary reaction. The hydrogenation activity of platinum under this condition was very low. Pt also improved the coke tolerance that the coke amount of Pt/HBeta was lower than the amount on HBeta. Krause et al. [109] performed guaiacol HDO experiment at 373 and 573 K and methyl transfer reaction was only observed under low temperature.

**Fig. 2** Difference between hydrogenolysis and hydrodeoxygenation [64]



Platinum was not effective in hydrogenation for all compounds. In the study by Liang et al. [110], platinum on silica-alumina neither hydrogenated the aromatic ring, nor removed the oxygen for benzofuran at 553 K. 2-methyl-2-pentenal is introduced as a special case here. Although it is not a model compound for lignin-derived bio-oil, it has C=O and C=C bonds. These two types of bonding existed in the bio-oil. In this compound, the two bonds are conjugated. Mallinson et al. [106] ran the experiment under 473 K and catalyzed by platinum on SiO<sub>2</sub>. Platinum showed high reactivity with the model compounds. The calculated rate constant showed that platinum mainly catalyze C=C bond. The reaction rate of C=O bond was much smaller. The preference for C=C hydrogenation was also reported in two other publications [111, 112]. By the way, the aliphatic –OH was cleaved under this condition.

Table 6 summarized the catalysts, reaction conditions, model compounds studied, and reaction type in this section. It is easy to find that temperature played a key role. Under 373–533 K, platinum mainly hydrogenates the aromatic structure. Almost all of the model compounds listed below are fully hydrogenated under this temperature. Deoxygenation occurs at temperature over 553 K. Krause et al. [109] performed guaiacol HYD/HDO experiment at 373 and 573 K. At 373 K, hydrogenated oxygen-containing compounds were the major product. When the temperature increased to 573 K, benzene became dominant product. It was explained that the higher temperature will suppress the hydrogenation reaction. The amount of hydrogen adsorbed on catalyst surface at different temperatures was proposed to be the major cause. Related study showed that hydrogen adsorption was exothermic reaction [113]. Low hydrogen coverage on catalysts at high temperature reduced reaction rate for both HYD and DO [109]. According to the experiment, the reaction rate of HYD was significantly reduced because it highly required more hydrogen than deoxygenation. On the other side, under higher pressure and lower temperature, it was more conducive to ring saturation [105].

How the model compounds interacting with catalyst surface directly determines the behavior of catalyst. Pt(111) are most stable facets of the Pt crystal [91]. Adsorption of

anisole and its derivatives on Pt [103] surface was studied [114]. The anisole was less strongly bonded to the surface compare to parent molecule benzene, probably due to the steric hindrance of the methoxy group. The most stable configuration was that the molecule adsorbed parallel to the surface with both aromatic ring and oxygen above the bridge sites. The binding energy for this configuration was 2.23 eV for Pt(111). Another vertical configuration resulted in a much weaker adsorption. The binding energy was only 1.09 eV. The adsorption on stepped surface was also studied because it was often considered as preferable sites for catalysis. The binding energy for Pt(211) was only 0.64 eV. The dissociation of phenol into phenoxy was endothermic on Pt(111) with reaction energy equal to 0.26 eV.

The addition of promoter is widely used to enhance the activity of the catalyst. Platinum and 3d metals showed superior performance than monometallic Pt in hydrogenation reaction [115, 116]. Adding Ni or Co into the Pt would not only increase the HDO activity, the distribution of products would be changed as well [102]. The deoxygenation selectivity is also higher on bimetallic catalysts, probably due to the additional sites generated. The EXAFS study showed that Pt-Ni and Pt-Co coordination number indicated the bimetallic formation well. If the number was greater than one, the Pt atom was surrounded by more Ni or Co atoms than Pt atoms. The DFT study [115–117] showed that Pt terminated surface bonded with hydrogen and hydrocarbon adsorbates more weakly than monometallic Pt surface, lead to optimized binding energies and higher rates of hydrogenation. Rh doping is also studied that PtRh improved the guaiacol conversion [109]. On the other hand, some dopant would cause adverse effect. For example, adding Pd into platinum catalyst might reduce guaiacol conversion due to the lowered active surface area [109].

### Palladium

Palladium is another widely used HDO catalyst. Under 423 K, Pd could hydrogenate phenol, anisole, catechol, and guaiacol effectively in water phase [118]. With the presence of phosphoric acid, the Pd/C converted phenolic and guaiacol-based compounds into aliphatic molecule in aqueous phase under 353 K.

**Table 6** Reaction condition for experiments using platinum catalyst

Model compounds (MC)	Temp	Hydrogen pressure		Support material	Solvent	Reaction type	Reference
		Absolute	H <sub>2</sub> to MC ratio				
Guaiacol, anisole, 4-methyl-anisole, cyclohexanone	573 K	0.14 MPa (30 % H <sub>2</sub> , 70 % N <sub>2</sub> )	–	γ-Al <sub>2</sub> O <sub>3</sub>	–	HYD <sup>a</sup> , HDO	[48]
Meta cresol	533 K	0.05 MPa	–	γ-Al <sub>2</sub> O <sub>3</sub>	–	HYD	[79]
Dibenzofuran	473 K	4 MPa	–	γ-Al <sub>2</sub> O <sub>3</sub> , ZSM-5, MZ-5(MS <sup>b</sup> )	Tridecane	HYD	[80]
Phenol	473–523 K	4 MPa	–	HY, ZSM-5, Hβ, γ-Al <sub>2</sub> O <sub>3</sub> , SiO <sub>2</sub>	Water	HYD, ring coupling	[81]
Guaiacol	523 K	4 MPa	–	γ-Al <sub>2</sub> O <sub>3</sub> , SiO <sub>2</sub> , NAC <sup>c</sup>	n-decane	Weak HYD	[82]
Anisole	673 K	0.1 MPa	50	SiO <sub>2</sub> , Hβ	–	HDO, HYD demethylation	[83]
4-Pr-Phenol	553 K	4 MPa	–	AC, ZrO <sub>2</sub> , TiO <sub>2</sub> , CeO <sub>2</sub>	Water	HYD, HDO	[85]
Guaiacol	373–573	8 MPa	–	ZrO <sub>2</sub>	Hexadecane	HYD Deoxygen	[87]
Benzofuran	553	3 MPa	–	SiO <sub>2</sub> -Al <sub>2</sub> O <sub>3</sub>	Decalin	HYD, HDO	[88]
2-methyl-2-pentenal	473	0.1 MPa	12	SiO <sub>2</sub>	–	HYD	[84]

<sup>a</sup> Hydrogenation<sup>b</sup> Mesoporous<sup>c</sup> Nitric-acid-treated carbon black

The turnover frequency (TOF) was very high (>1,000 h<sup>-1</sup>) and the recyclability was excellent that no deactivation observed after 6 h [119]. For the phenolic dimers connected in various bonding (including α-O-4, 4-O-5, β-1, 5-5, β-β), the Pd/C and solid acid HZSM-5 achieved 100 % hydrogenation and deoxygenation at 473 K in water phase [120].

The behavior of palladium is similar to platinum therefore they were compared in some study. The activity of these two catalysts highly depended on the reaction condition. In Liang et al.'s study [110], metal dispersion of Pd was only half as the value on Pt, but the CO uptake amount was 50 % higher than it was on Pt and Pd catalyst also showed higher activity than Pt in the both hydrogenation and HDO of benzofuran. The study indicated that the HYD of benzofuran and the cleavage of C-O were easier over Pd than Pt. In some other cases, Pt showed better performance than Pd. In the HDO of 4-propyl-phenol under 553 K in acid-free aqueous solution, Pd on active carbon was used as catalyst [107]. Pd was good at hydrogenation but not at hydrogenolysis of C-O bond compared with Pt, Ru, and Rh. More than half of the aliphatic -OH was left uncleaved. Another example was that under 373 K and 8 MPa H<sub>2</sub>, Pd was not effective in either HYD or HDO of guaiacol. Half of the methoxy group was removed under this condition [109].

Understanding how the metal dispersed in the support material is a big help in catalyst optimization. In the study by Suzuki et al. [121], CeO<sub>2</sub> and ZrO<sub>2</sub> was used as support. The amount of H<sub>2</sub> chemisorbed as well as Pd metal surface

area increased abruptly when Pd loading increased from 1 to 3 wt.%. On the other hand, the Pd crystallite size increased almost linearly. These two means that (1) deposition was more on external surface as the loading increase, (2) Pd first preferentially occupied the internal surface. The increasing in the Pd loading increased the d-spacing of CeO<sub>2</sub> mesoporous structure, which meant Pd particles expanded the pore structure. For CeO<sub>2</sub> support, the increasing loading led to higher conversion but lower TOF value [121]. When Pd loading is low, more C-hexanone was produced. When Pd loading was high, more hexanol and hexane were produced. The temperature effect was also studied. Under 333 K, the conversion was highest. The overall conversion decreased monotonously with increasing temperature. Other two researchers also found the max conversion at 433 K [122, 123]. When the temperature went higher, more cyclohexane and cyclohexanone and less cyclohexanol were produced [121, 124]. For ZrO<sub>2</sub> support, the result was much simpler that the conversion of phenol was similar to the conversion on Pd/CeO<sub>2</sub> and the selectivity to cyclohexanone was above 90 %.

Pd<sub>4</sub>Pt<sub>1</sub> was made to study the alloy effect [110]. The dispersion was doubled than Pd monometallic catalyst and the CO uptake amount was also doubled. The selectivity of Pd<sub>4</sub>Pt<sub>1</sub> towards deoxygenated products was 80 %, compared with Pd monometallic catalyst was 37 %. The TOF of Pd<sub>4</sub>Pt<sub>1</sub> was 16.88, which was much higher than the TOF of Pd 2.15. The surface change of Pd after alloying with Pt is

summarized as (1) bonding length of Pd, (2) electronic density in Pd. From the CO chemisorption change, these factors enhanced the exposure of active sites on catalyst surface.

Orita and Itoh studied phenol the formation of phenol from benzene on the surface on Pd(111) [125]. Pd(111) was the most stable facet for palladium. Even in polycrystalline Pd, it was still most abundant. The deoxygenation was basically the reverse for this reaction. The adsorption of phenol on Pd surface was less stable than benzene. The adsorption energy of phenol on Pd(111) was  $-7.85$  eV. When one hydrogen atom attached to the C-1, the adsorption energy of the intermediate increased to  $-6.85$  eV. Then the O-atom and benzene were both adsorbed on one unit cell. The co-adsorption system becomes more stable ( $-7.06$  eV). The last step is C-O bond cleavage. The sum of adsorption energies of oxygen atom and benzene in separate domains is  $-7.26$  eV, with benzene adsorption energy at  $-1.43$  eV and oxygen adsorption energy at  $-5.83$  eV.

### Rhodium

Rhodium was a relatively newly developed catalyst compared with platinum and palladium catalysts. However, it showed excellent performance in some cases. Under 553 K in acid-free aqueous solution, rhodium on activated carbon successfully catalyzed the HDO reaction of 4-propyl-phenol [107]. The conversion of reactant was 100 and 83 % aliphatic  $-OH$  was cleaved. The hydrogenation of guaiacol occurred on metal at 331–381 K and the deoxygenation occurred over 523 K [104]. Both temperatures were lower than the temperature required by platinum, which indicated the high reactivity of Rh in HDO experiment. In another guaiacol HDO experiment under 373 K, the main product with Rh catalyst was 1-methyl-1,2-cyclohexanediol [109]. The conversion was 100 % on HYD. However, it did not effectively achieve C-O hydrogenolysis. Rh showed better performance than Pt and Pd in hydrogenation under the same condition, probably due to the high amount of irreversible chemisorption of  $H_2$  on the Rh surface.

The temperature effect on guaiacol HDO was also studied for Rh catalyst [96]. The temperature range studied was 573–673 K. The increasing temperature led to higher cyclohexane yield. The coke formed on Rh decrease with the increasing temperature. The  $C_xH_yO_2$  compound decreased dramatically in the temperature range (especially increased from 623 to 673 K). Both mono-oxygen compound and aliphatic compound increased. At 673 K, the aliphatic yield was almost 50 %. RhPt and RhPd were both synthesized for comparison and monometallic Rh catalyst had the highest HDO reactivity than both of them.

Rh(111) is the most stable facets of rhodium [91]. Phenol showed strong adsorption on Rh(111) with binding energy of 2.79 eV under horizontal configuration. Under vertical

configuration, the binding energy was 1.15 eV, which was much weaker than the energy from horizontal configuration. On the stepped surface Rh(211), the binding energy reduced to 1.79 eV. The dissociation of phenol to phenoxy was  $-0.27$  eV, which indicated an exothermic reaction. However, for finite coverage, the dissociation on Rh(111) required lower temperature than it was on Pt(111) [126, 127].

### Ruthenium

Ruthenium on activated carbon was used to catalyze the HDO of 4-propyl-phenol under 553 K in acid-free aqueous solution [107]. In the study, ruthenium catalyst achieved 100 % hydrogenation but the deoxygenation capability was weaker than Rh and Pt that only 50 % aliphatic  $-OH$  bond was cleaved.

The performance of ruthenium is highly affected by the support. Although it is also observed for other metal catalysts, the effect is stronger for ruthenium. In the study by Park et al. [104], platinum, rhodium, palladium, and ruthenium were compared in guaiacol HDO on three different support materials. When using  $\gamma-Al_2O_3/SiO_2-Al_2O_3$ /nitric acid treated carbon black as supports, the highest product yield were cyclohexanol/cyclohexane/2-methoxycyclohexanol, respectively. Furthermore, the selectivity of the ruthenium was the best among Pt, Pd, Rh, and Ru.

The HDO of phenol and anisole by using Ru/charcoal were studied by Kluson and Cervený [128]. The reaction network was proposed and kinetics data was calculated. The reaction network will be discussed in detail in [Source of Hydrogen and Economic Analysis](#) section. The result indicated that ruthenium was able to remove the aliphatic  $-OH$  and aliphatic methoxy through dehydration. When there was a carbonyl group attached to the aromatic ring, the C=O bond was hydrogenated first, then the hydrogenation of aromatic ring happened.

Zhang et al. studied the hydrotreating of eugenol by using ruthenium catalyst [129]. The major crystal facet of ruthenium was Ru(101) and the major facet of Pd is Pd(111). Under similar condition, ruthenium showed much higher activity than palladium, which was in accordance with the study by Greenfield [130]. The reactivity of catalyst had no loss after two runs with model compounds. When using distilled fraction from bio-oil as reactant (major components were phenolic compounds, such as phenol, 2-methoxyphenol, 4-ethylphenol, 4-methyl-2-methoxyphenol, and 4-ethyl-2-methoxyphenol), the catalyst lost activity rapidly. The BET study showed the reduction in both surface area and pore volume, which indicated the coke or tar formation in pore channels. The study further revealed that  $Ru^0$  were the major role in HYD reaction.

Heeres et al. studied the hydrotreatment of fast pyrolysis oil using Ru/C at 623 K and 20 MPa  $H_2$  pressure [72]. The ruthenium catalyst was very effective in deoxygenation in

the beginning. After 1 h, the O/C molar ratio decreased from 0.45 to 0.02. However, with the time going, it increased from 0.02 to 0.07 from 1 to 6 h reaction time. Probably due to the low O/C ratio compounds transferred from oil phase to gas phase. The H/C ratio was 1.35 for the pyrolysis oil. At 1 h, it dropped to 1.05 at first, and then increased to 1.32 after 6 h. The initial drop was probably caused by loss of hydrogen for dehydration.

### Support Effect

The acidity is the key feature of support material. Acid sites on HBeta are well known for catalyzing alkyl transfer reaction [71]. In the paper by Resasco et al., the intermolecule methyl transfer was observed. When SiO<sub>2</sub> was used as the support, the methyl group was rapidly hydrogenated to form methane. This result meant that the methyl group was stable on the zeolite surface but unstable on SiO<sub>2</sub> surface. Not only HBeta zeolite, both  $\gamma$ -Al<sub>2</sub>O<sub>3</sub> [64] and HY zeolite [131, 132] induced the intramolecule- and intermolecule-methyl group transfer reaction. Especially for HY zeolite catalyst, transalkylation was the only kinetically significant reaction class. Besides catalyzing alkyl transfer reaction, acid site affected the rate of dehydration. Under 373 K, ZrO<sub>2</sub> could not dehydrate the cyclohexanol produced by guaiacol. Methyl transfer was observed in this reaction [109]. HY zeolite was also used and the presence of acid protons for dehydration was necessary for deoxygenation of aliphatic -OH [103]. Furthermore, the selectivity to bicyclics with HY and H $\beta$  zeolite-supported catalyst was higher than over HZSM-5 because of the micropores and shape-selective effects.

Acid support material sometimes shows synergetic effect with the metal. In the study by Ha et al. [104], Rh/Al has ten times more active sites compared to Rh/SiAl. However, Rh/SiAl exhibited much better HDO activity. Even mechanical mix of metal-deposited non-acid support and noble-metal-free SiAl could also enhance the deoxygenation ability. When using Pt/ZrO<sub>2</sub> as the catalyst, only negligible deoxygenated products were produced.

Besides using acid site on support, the mineral acid could also reach similar effect. For example, sulfated zirconia, Amberlyst 15, Nafion/SiO<sub>2</sub>, and Cs<sub>2.5</sub>H<sub>0.5</sub>PW<sub>12</sub>O<sub>40</sub> could all lead to 90 % yield of cycloalkanes with the presence of noble metal catalyst mentioned in aqueous phase HDO [120]. The activation energy for these five solid acids was normally below 120 kJ/mol, which was almost equal to the activation energy of H<sub>3</sub>PO<sub>4</sub> in water. HZSM-5 is a special case. With Si/Al ratio of 45, HZSM-5 produced 93 % cycloalkanes due to the lower activation energy of dehydration (approximately 95 kJ/mol). Therefore, HZSM-5 could dehydrate under lower temperature.

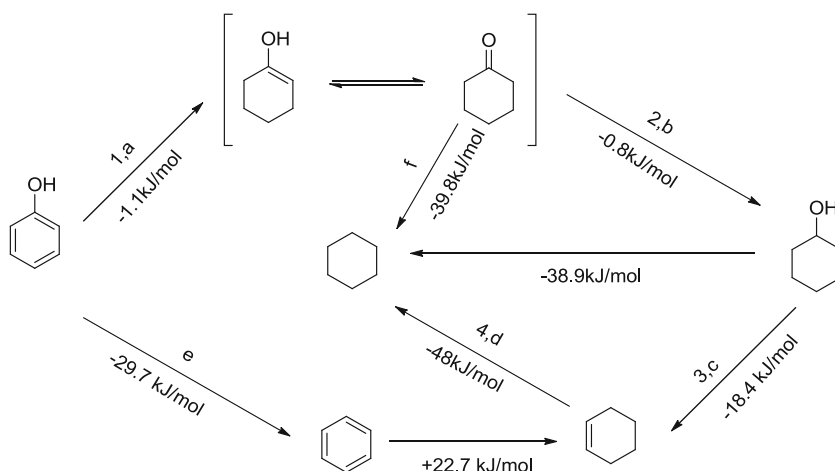
The acid site on support would further affect the interaction between reactant and support material. Chemisorption of

guaiacol was tested on ZrO<sub>2</sub> and  $\gamma$ -Al<sub>2</sub>O<sub>3</sub> supports [96]. There was no special response on desorption of guaiacol on  $\gamma$ -Al<sub>2</sub>O<sub>3</sub> surface. ZrO<sub>2</sub> exhibited at least three peaks in the desorption profile. The total area for ZrO<sub>2</sub> had larger area than  $\gamma$ -Al<sub>2</sub>O<sub>3</sub>. This indicated that the bonding strength between guaiacol and ZrO<sub>2</sub> was weaker than the bonding strength between guaiacol and  $\gamma$ -Al<sub>2</sub>O<sub>3</sub>. The acid strength of  $\gamma$ -Al<sub>2</sub>O<sub>3</sub> was stronger than ZrO<sub>2</sub>. This proved that the higher acid strength had stronger bonding with the model compound. In another study [99], ZrO<sub>2</sub> showed better catalytic activities towards C<sub>arom</sub>-O hydrogenolysis through demethoxylation and direct deoxygenation than TiO<sub>2</sub> and Al<sub>2</sub>O<sub>3</sub>.

Not only the acid strength, the porous structure affects the activity of the catalyst as well. The high porous diameter increases the diffusion rate of model compounds inside the catalyst. As mentioned above, zeolites are better support than alumina and silica in phenol HDO since zeolites have stronger acidity. However, small pore size causes diffusion limitation, especially for the large compound [103]. Therefore mesoporous zeolite is the ideal material, since it has the advantage of zeolites and ordered mesoporous material. In this paper, the MZ-5 possessed intracrystalline wormhole mesopore channels. In following study, it was proved that the reaction rate was increased due to the increase diffusion rate. 2M2P isomerization was a model reaction to test the acidity of the catalyst and the result showed that MZ-5 and ZSM-5 had higher acidity than  $\gamma$ -Al<sub>2</sub>O<sub>3</sub>. For Pt/ $\gamma$ -Al<sub>2</sub>O<sub>3</sub>, high Pt dispersion and mesoporous nature made it to have high HYD ability but mild acidity limited the dehydration. Pt/ZSM-5 had limited hydrogenation ability due to the small pore size. Overall speaking, MZ-5 had high reaction rate in hydrogenation and dehydration.

Suzuki et al. [121] compared the reactivity of Pd deposited on MgO,  $\gamma$ -Al<sub>2</sub>O<sub>3</sub>, mesoporous CeO<sub>2</sub>, and mesoporous ZrO<sub>2</sub>. Pd/MgO was very active and selective for cyclohexanone. However, MgO had very poor mechanical strength, which inhibited it from being used in industrial scale.  $\gamma$ -Al<sub>2</sub>O<sub>3</sub> was least active but most selective. Mesoporous CeO<sub>2</sub> and mesoporous ZrO<sub>2</sub> were equally active. Higher catalytic activity of mesoporous supports compared to that of the commercial microporous supports was attributed to higher palladium surface area, higher dispersion, and smaller crystallite size due to the higher BET surface area on mesoporous system. Pure CeO<sub>2</sub> possessed weak acid and a weak base. ZrO<sub>2</sub> was relatively strong acid and strong base, compared to CeO<sub>2</sub>. When heat up between 473 and 673 K, the surface reduction of CeO<sub>2</sub> began and it became CeO<sub>2-x</sub>/Ce<sub>2</sub>O<sub>3</sub>-like non-stoichiometric oxide with anion vacancies, thus Lewis acidic and basic sites were formed. Phenol adsorbed in non-planar fashion. The redox property of CeO<sub>2</sub> also facilitated the alkylation of phenol with propanol [133]. ZrO<sub>2</sub> was not easily

**Fig. 3** Reaction network proposed for phenol HDO and the calculation of Gibbs energy in each step [121]



reducible. Hydrogen was adsorbed dissociatively to form Zr-OH, Zr-H, and ZrHZr [134] that the surface hydroxyl group could have acidic or basic character with Bronsted centers depending on the polarization of the OH group. Carbon deposition during alkylation and hydrogenation of phenol on these Bronsted center caused the activity decay [135, 136].

The structure change of the support material during the reaction is one of the major causes for catalyst deactivation, especially when using water as solvent. Both SiO<sub>2</sub> and γ-Al<sub>2</sub>O<sub>3</sub> are tentatively to degrade under water and water vapor. In the study by Aprile et al. [137], the pore structure in SiO<sub>2</sub> support was collapsed after the reaction in aqueous phase, which led to complete deactivation of catalyst. The solubility of amorphous silica in water was also measured but the amount is relatively minor [138]. The transformation of γ-alumina was investigated by Lefevre et al. [139]. The study revealed that γ-alumina transformed to bayerite (β-Al(OH)<sub>3</sub>) gradually with the presence of water and most of the acidity sites were disappeared, which result in the low reactivity of the catalyst.

### Mechanism and Kinetic Study

#### Phenolic-Based Compound

Phenol was the most commonly studied model compounds in lignin-derived bio-oil upgrading [91, 103, 107, 118, 119, 121]. It was the simplest compound which consisted aromatic structure and phenolic oxygen. The study of phenol can reveal the fundamental reaction mechanism of other related compound.

In the study by Lercher et al. [118, 119], the reaction path was proposed as follows: (1) aromatic ring was partially hydrogenated to cyclohexanone or fully hydrogenated to cyclohexanol, (2) the cyclohexanone was further hydrogenated to cyclohexanol, (3) the -OH on cyclohexanol was removed through dehydration, and (4) the C=C double bond was finally hydrogenated and cyclohexane was produced. The authors believed that the phenol and cyclohexanol could not be directly deoxygenated. These reactions were marked in (1)–(4) in Fig. 3.

Jones et al. proposed another reaction pathway in phenol HDO [103], (a) phenol were converted into cyclohexenol as an intermediate product, (b) the cyclohexenol was converted

**Fig. 4** Reaction path of anisole HDO on (a) only acid site, (b) only metal, and (c) metal and acid site [105]

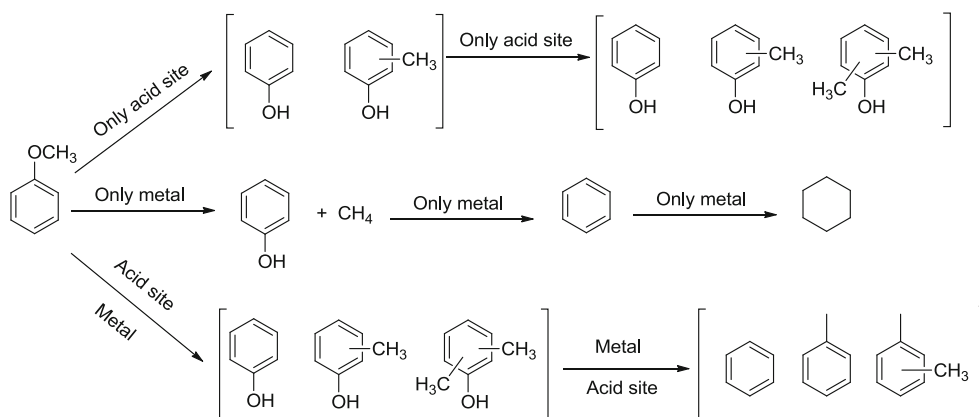
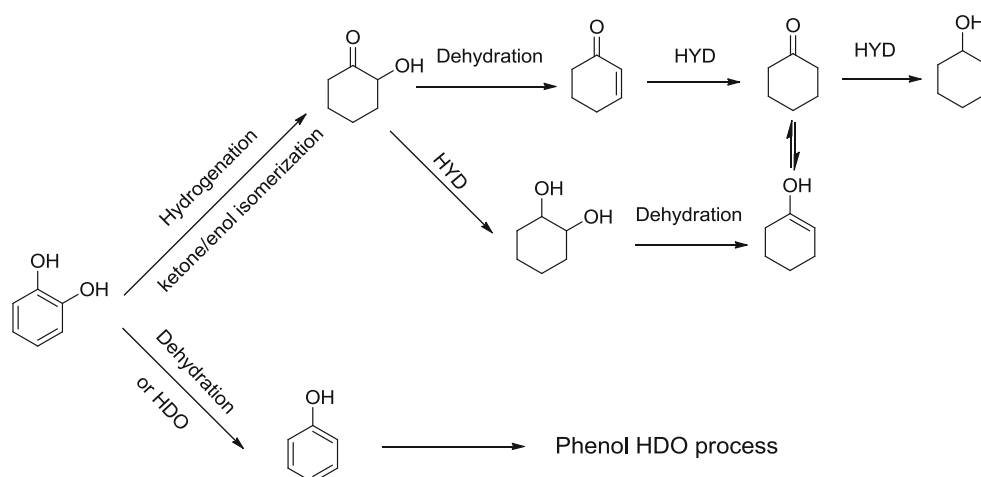


**Fig. 5** Reaction path of catechol HDO [118]



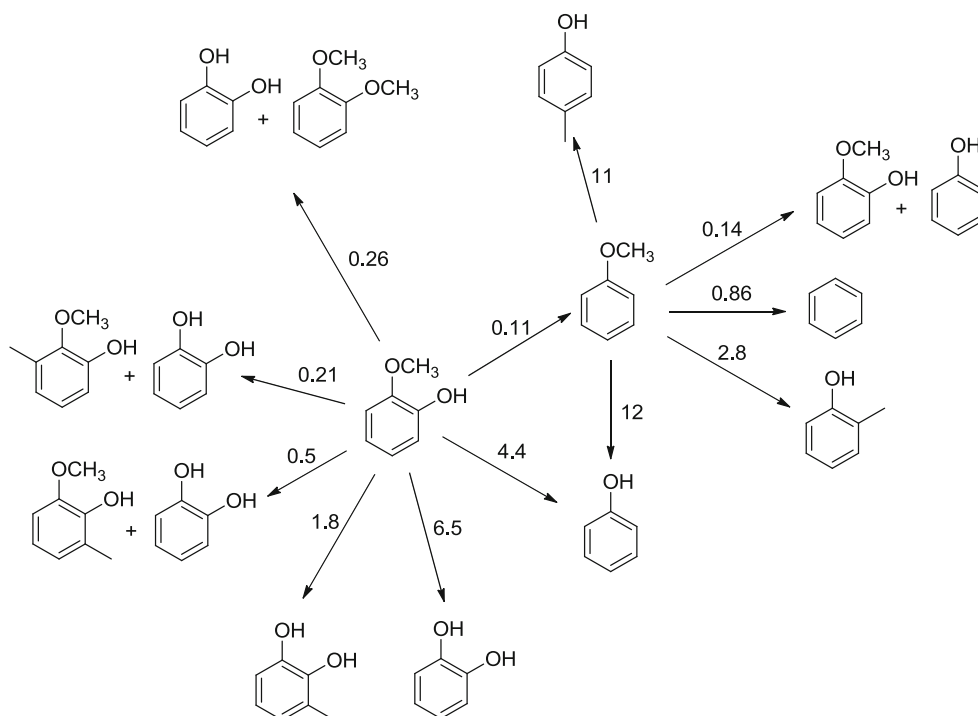
to cyclohexanone or further hydrogenated to cyclohexanol, (c) cyclohexanol was dehydrated to cyclohexene, and (d) cyclohexene was finally hydrogenated to cyclohexane. Two extra proposed steps were (e) phenol directly HDO to form benzene and (f) cyclohexone converted to cyclohexane in one step through hydrogenolysis. These reactions were marked in (a)–(f) in Fig. 3.

The Gibbs energy in each step for phenol HDO was calculated by Keane et al. under 498 K [136]. The values were listed below the arrow in Fig. 3 and the unit was kJ/mol. Except the partial HYD of benzene to cyclohexene, the standard free energies of all other HYD/hydrogenolysis reactions were negative. Therefore all hydrogenolysis steps and the benzene hydrogenation steps were considered to be

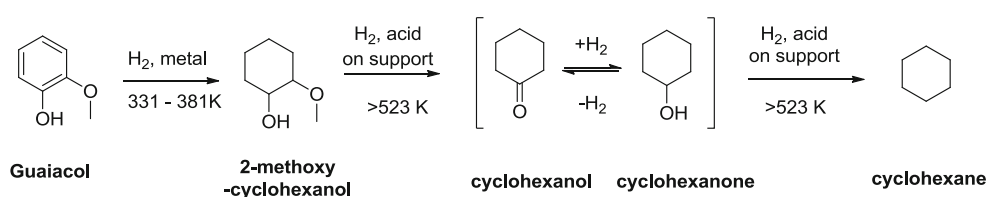
irreversible. Cyclohexanone was produced by hydrogenation of cyclohexenol followed by a tautomerism, but the Gibbs energy was not able to be calculated due to the missing of thermochemical data for this reaction.

How the phenol adsorbed on the catalyst surface was also calculated [91]. After phenol was adsorbed on the metal surface, the C–C bond was slightly stretched, which make it more to  $sp^3$  hybrid than  $sp^2$  hybrid. The C–O bond was slightly shifted away from the horizontal benzene and the bonding length was also increased. These changes increased the reactivity of C=C and C–O bond and made the hydrogenation and HDO reaction became possible. Suzuki et al. [121] studied the formation of cyclohexanone and cyclohexanol from benzene. The result suggested that the selectivity to cyclohexanone or cyclohexanol

**Fig. 6** Part of the reaction network for guaiacol HDO by Pt/ $\gamma$ - $Al_2O_3$  at 534 K and 140 kPa  $H_2$  proposed by Gates et al. [64]. Experimentally calculated rate constant had unit in  $L(g\text{catalyst})^{-1}h^{-1}$





**Fig. 7** Reaction path proposed by Park et al. [104]

depended on the configuration of phenol adsorption on metal surface. Cyclohexanone was produced if phenol was adsorbed non-planar to the surface. If the phenol was adsorbed co-planar to the surface, cyclohexanol was the product. The modes of adsorption of phenol were governed by the nature of the support, mainly the acid–base properties [123, 135].

#### Anisole-Based Compounds

Compared with phenol, anisole has one more methyl group attached to the oxygen. The methyl transfer from the methoxyl to aromatic ring makes it different from phenol in HDO experiment. Resasco et al. observed that the acidic function catalyzed the transalkylation reaction, yielding phenol, cresols, and xylenols as major products [105]. The reaction was done in gas phase under 673 K and atmospheric hydrogen pressure. The noble metal catalyst was able to cleave the PhO-CH<sub>3</sub> bond and form phenol and methane. The phenol part was further hydrodeoxygenated and form benzene or cyclohexane. The presence of noble metal and acid support also had synergistic effect that the methyl group was transferred to the aromatic ring first, then the HDO reaction occur, which reduced the carbon loss as methane. The reaction path was shown in Fig. 4.

With the existence of water, the reaction path was slightly different. Methanol was produced instead of methane above through acid hydrolysis [118]. Weckhuysen et al. did the HDO on anisole under 573 K and 5.0 MPa hydrogen pressure [97]. The selectivity from anisole towards phenol and phenol with methyl substituted on aromatic ring were >35 % and 10–35 %, respectively.

#### Catechol-Based Compounds

Two major reaction paths for catechol were (a) hydrogenation first, then go through HDO and (b) removal of one hydroxyl group first, then go through reaction as phenol [97, 118]. The reaction path was drawn in Fig. 5. Under 473 K and 5.0 MPa hydrogen pressure, the selectivity of catechol towards 2-hydroxycyclohexanone were 80 % in water phase [118]. The following dehydration of 2-hydroxycyclohexanone was very fast under acid condition and cyclohexanone was formed rapidly via two parallel reactions. The major path was ketone hydrogenation and alcohol dehydration.

#### Guaiacol-Based Compound

Guaiacol is the most representative model compound for lignin-derived bio-oil. Compared to phenol, there is one more methoxy group attached to the aromatic ring. This small change makes the reaction network of guaiacol much more complex than the phenol. During the reaction, HDO, hydrogenolysis, transalkylation, bimolecular transalkylation, and hydrogenation are all observed [64]. The complete reaction network is shown in Fig. 6 and the reaction rate constants are marked next to the arrow. Only part of the reaction was listed.

We can draw following conclusion from the information above.

1. The methyl group in the guaiacol is very unstable. The acid support can transfer the methyl intermolecularly or intramolecularly. The transferred methyl group attaches to the aromatic ring and phenolic oxygen.
2. The methoxy or hydroxyl group on the guaiacol is cleaved in one step. Both products can be further HDO to form benzene.
3. Guaiacol cannot be hydrogenated in one step under this condition. Normally it is converted to anisole or phenol first, and then the aromatic ring is hydrogenated.
4. The cyclohexane is produced in two major routes. First is from the hydrogenation of phenol, which is the product of HDO of guaiacol. Second is the hydrogenolysis of cyclohexanol and cyclohexanone.

In the study by Park et al. [104], the reaction path was proposed as Fig. 7. The major difference compared with the reaction network above was that guaiacol was directly hydrogenated to form 2-methoxy-cyclohexanol under 331–381 K. Then the methoxy was removed by acid site on support. In the last step, the cyclohexane was produced by dehydration of cyclohexanol and cyclohexanone. The acid catalyst and temperature above 523 K were two necessary conditions for demethoxy and dehydration reaction.

#### Conclusion

Owing to the complicated components, chemical analysis of pyrolysis oil has been a challenging but crucial undertaking. GC-MS analysis has always been used to analyze individual components in pyrolysis oil, however, only a small portion

could be detected by GC due to the poor volatility. The spectroscopic technique such as FT-IR could give insights into the whole portions of pyrolysis oil. Unfortunately, the ability of such method to deal with complex mixture like pyrolysis oil is very limited. As a new way introduced into characterization of pyrolysis oil—NMR has some advantages compare to the traditional methods. NMR has the ability to analyze the whole portion of pyrolysis oil. In addition, it could characterize more than 30 different functional groups present in the lignin pyrolysis oil and give quantitative results; nevertheless NMR could not provide exact structure of the components, which still make it difficult (or impossible) to complete chemical characterization of pyrolysis oil.

The upgrading of the lignin-derived pyrolysis oil is reviewed in terms of the common catalyst and reaction mechanism of key model compounds. It is shown that both sulfided catalysts and noble metal catalysts have advantages and disadvantages. Sulfided catalyst is intensively studied and the cost is relatively cheap. The reaction is done under atmospheric pressure with excellent HDO capacity under gas phase. However, the severe coke formation, intolerant to water and environment contamination for sulfur leaching cause big problem. On the other hand, noble metal catalyst shows higher reactivity for hydrogenation under either gas phase or water phase. The reusability of noble metal catalyst is better than sulfided catalyst. The reaction needs lower temperature. But the noble metal catalyst can be easily poisoned by sulfur and the high cost also hinders it from real application.

The choosing of support greatly changes the reaction path. On one hand, the small opening of zeolite might cause some diffusion problem and lower the reactivity. On the other hand, it also increases the selectivity. Zeolite modification into mesoporous structure significantly increased the reactivity. The dehydration and transalkylation reaction mainly occur on the acid site. Too strong acidity or bonding with reactant reduces the desorption rate and lower the reaction rate. The stability of catalyst support materials requires special attention because it would affect the reactivity and durability of catalyst. Acidity and surface area are two key parameters for support material characterization.

The performance of catalysts varies with different feeding stocks. Overall speak, according to the publications involved in this paper, the order of metal sites activity is  $Rh \sim Ru > Pt > Pd$ . Again, it is not strictly follow this order for all starting material. Rhodium and ruthenium showed obvious higher reactivity in HYD than platinum and palladium in most case. Rhodium also has showed high deoxygenation ability. Ruthenium was not as good as platinum for deoxygenation in model compound study. But when the feedstock changed to the pyrolysis oil, it removed oxygen intensively. Plus the acid support would greatly enhance the deoxygenation ability through acid dehydration under even lower temperature than

the temperature required for deoxygenation through hydrogenolysis. Zeolite material could be a promising candidate due to the tunable acidity and pore size. The thermal/water vapor stability is the major concern in this specific application.

The reaction condition greatly impacts the result. Both types of catalysts showed similar ability in HDO and HYD. The main difference is selectivity. Generally speaking, higher reaction temperature favors HDO and lower temperature favors HYD. It is because of the amount of hydrogen adsorbed on catalyst is lower under high temperature that HYD reaction requires large amounts of hydrogen. The solvent effect and other parameters varied. Hydrolysis is an important reaction to consider when the reaction is done under water phase.

The four model compounds for mechanism study in this paper are phenol, anisole, catechol, and guaiacol. These four compounds are chosen based on the component study in [Source of Hydrogen](#) and [Economic Analysis](#) section. The main reactions involved are HYD and HDO. Transalkylation and ring-coupling reaction are also observed.

## Reference

1. Perlack RDW, L. L.; Turhollow, A. F.; Graham, R. L.; Stokes, B. J.; Erbach, D. C., (2005). Biomass as Feedstock for a bioenergy and bioproducts Industry: the technical feasibility of a billion-ton annual supply. Technical Report by ORNL, Apr 2005
2. Administration EI (June 2012) Monthly Energy Review. US Department of Energy
3. Administration-0384 EI (2011) Annual Energy Review 2010. Department of Energy
4. Franks JR, Hadingham B (2012) Reducing greenhouse gas emissions from agriculture: avoiding trivial solutions to a global problem. *Land Use Policy* 29(4):727–736
5. Iribarren D, Peters JF, Dufour J (2012) Life cycle assessment of transportation fuels from biomass pyrolysis. *Fuel* 97:812–821
6. van Oort PAJ, Timmermans BGH, van Swaaij ACPM (2012) Why farmers' sowing dates hardly change when temperature rises. *Eur J Agron* 40:102–111
7. Lenzen M, Schaeffer R (2012) Historical and potential future contributions of power technologies to global warming. *Clim Change* 112(3):601–632
8. Biasutti M, Sobel A, Camargo S, Creyts T (2012) Projected changes in the physical climate of the Gulf Coast and Caribbean. *Clim Change* 112(3):819–845
9. Climate Change 2007: Synthesis Report (2007). Intergovernmental Panel on Climate Change
10. Zakzeski J, Bruijninx PCA, Jongerius AL, Weckhuysen BM (2010) The catalytic valorization of lignin for the production of renewable chemicals. *Chem Rev* 110(6):3552–3599
11. Parikka M (2004) Global biomass fuel resources. *Biomass Bioenergy* 27(6):613–620
12. Ragauskas AJ, Williams CK, Davison BH, Britovsek G, Cairney J, Eckert CA, Frederick WJ Jr, Hallett JP, Leak DJ, Liotta CL, Mielenz JR, Murphy R, Templer R, Tschaplinski T (2006) The path forward for biofuels and biomaterials. *Science* 311(5760):484–489
13. Jones S, Elliott DC, Kinchin C, Valkenburg C, Holladay J, Czemik S, Walton C, Stevens D (2009) Design case

- summary—production of gasoline and diesel from biomass via fast pyrolysis, hydrotreating and hydrocracking. US Department of Energy
14. Mohan D, Pittman CU, Steele PH (2006) Pyrolysis of wood/biomass for bio-oil: a critical review. *Energy Fuel* 20(3):848–889
  15. Anex RP, Aden A, Kazi FK, Fortman J, Swanson RM, Wright MM, Satrio JA, Brown RC, Daugaard DE, Platon A, Kothandaraman G, Hsu DD, Dutta A (2010) Techno-economic comparison of biomass-to-transportation fuels via pyrolysis, gasification, and biochemical pathways. *Fuel* 89 Suppl 1:S29–S35
  16. Caballero JA, Font R, Marcilla A (1996) Study of the primary pyrolysis of Kraft lignin at high heating rates: yields and kinetics. *J Anal Appl Pyrolysis* 36(2):159–178
  17. Caballero JA, Font R, Marcilla A (1997) Pyrolysis of Kraft lignin: yields and correlations. *J Anal Appl Pyrolysis* 39(2):161–183
  18. Caballero JA, Font R, Marcilla A, García AN (1993) Flash pyrolysis of Klason lignin in a Pyroprobe 1000. *J Anal Appl Pyrolysis* 27(2):221–244
  19. Ferdous D, Dalai AK, Bej SK, Thring RW (2002) Pyrolysis of lignins: experimental and kinetics studies. *Energy Fuel* 16(6):1405–1412
  20. Ferdous D, Dalai AK, Bej SK, Thring RW, Bakhshi NN (2001) Production of H<sub>2</sub> and medium Btu gas via pyrolysis of lignins in a fixed-bed reactor. *Fuel Process Technol* 70(1):9–26
  21. Iatridis B, Gavalas GR (1979) Pyrolysis of a precipitated Kraft lignin. *Ind Eng Chem Prod RD* 18(2):127–130
  22. Nunn TR, Howard JB, Longwell JP, Peters WA (1985) Product compositions and kinetics in the rapid pyrolysis of milled wood lignin. *Ind Eng Chem Process Des Dev* 24(3):844–852
  23. Ben H, Ragauskas AJ (2012) Torrefaction of Loblolly pine. *Green Chem* 14(1):72–76
  24. Sharma RK, Hajaligol MR (2003) Effect of pyrolysis conditions on the formation of polycyclic aromatic hydrocarbons (PAHs) from polyphenolic compounds. *J Anal Appl Pyrolysis* 66:123–144
  25. Sharma RK, Wooten JB, Baliga VL, Lin X, Geoffrey Chan W, Hajaligol MR (2004) Characterization of chars from pyrolysis of lignin. *Fuel* 83(11–12):1469–1482
  26. Hosoya T, Kawamoto H, Saka S (2009) Role of methoxyl group in char formation from lignin-related compounds. *J Anal Appl Pyrolysis* 84(1):79–83
  27. Chu S, Subrahmanyam AV, Huber GW (2013) The pyrolysis chemistry of a [small beta]-O-4 type oligomeric lignin model compound. *Green Chem* 15(1):125–136
  28. Asmadi M, Kawamoto H, Saka S (2011) Gas- and solid/liquid-phase reactions during pyrolysis of softwood and hardwood lignins. *J Anal Appl Pyrolysis* 92(2):417–425
  29. Chen H-W, Song Q-H, Liao B, Guo Q-X (2011) Further separation, characterization, and upgrading for upper and bottom layers from phase separation of biomass pyrolysis oils. *Energy Fuel* 25(10):4655–4661
  30. Hosoya T, Kawamoto H, Saka S (2009) Solid/liquid- and vapor-phase interactions between cellulose- and lignin-derived pyrolysis products. *J Anal Appl Pyrolysis* 85(1–2):237–246
  31. Hyder M, Jönsson JÅ (2012) Hollow-fiber liquid phase microextraction for lignin pyrolysis acids in aerosol samples and gas chromatography–mass spectrometry analysis. *J Chromatogr A* 1249:48–53
  32. Jiang G, Nowakowski DJ, Bridgwater AV (2010) Effect of the temperature on the composition of lignin pyrolysis products. *Energy Fuel* 24(8):4470–4475
  33. Lou R, S-b W, G-j L (2010) Effect of conditions on fast pyrolysis of bamboo lignin. *J Anal Appl Pyrolysis* 89(2):191–196
  34. Lou R, Wu S-B, Lv G-J, Guo D-L (2010) pyrolytic products from rice straw and enzymatic/mild acidolysis lignin. *BioRes* 5(4):2184–2194
  35. Mullen CA, Boateng AA (2010) Catalytic pyrolysis-GC/MS of lignin from several sources. *Fuel Process Technol* 91(11):1446–1458
  36. Patwardhan PR, Brown RC, Shanks BH (2011) Understanding the fast pyrolysis of lignin. *ChemSusChem* 4(11):1629–1636
  37. Yang Q, Wu S, Lou R, Lv G (2010) Analysis of wheat straw lignin by thermogravimetry and pyrolysis–gas chromatography/mass spectrometry. *J Anal Appl Pyrolysis* 87(1):65–69
  38. Bocchini P, Galletti GC, Camarero S, Martinez AT (1997) Absolute quantitation of lignin pyrolysis products using an internal standard. *J Chromatogr A* 773(1–2):227–232
  39. Greenwood PF, van Heemst JDH, Guthrie EA, Hatcher PG (2002) Laser micropyrolysis GC–MS of lignin. *J Anal Appl Pyrolysis* 62(2):365–373
  40. Ingram L, Mohan D, Bricka M, Steele P, Strobel D, Crocker D, Mitchell B, Mohammad J, Cantrell K, Pittman CU (2008) Pyrolysis of wood and bark in an auger reactor: physical properties and chemical analysis of the produced bio-oils. *Energy Fuel* 22(1):614–625
  41. Jegers HE, Klein MT (1985) Primary and secondary lignin pyrolysis reaction pathways. *Ind Eng Chem Proc RD* 24(1):173–183
  42. Nowakowski DJ, Bridgwater AV, Elliott DC, Meier D, de Wild P (2010) Lignin fast pyrolysis: results from an international collaboration. *J Anal Appl Pyrolysis* 88(1):53–72
  43. Scholze B, Meier D (2001) Characterization of the water-insoluble fraction from pyrolysis oil (pyrolytic lignin). Part I. PY–GC/MS, FTIR, and functional groups. *J Anal Appl Pyrolysis* 60(1):41–54
  44. Saiz-Jimenez C, De Leeuw JW (1986) Lignin pyrolysis products: their structures and their significance as biomarkers. *Org Geochem* 10(4–6):869–876
  45. Scholze B, Hanser C, Meier D (2001) Characterization of the water-insoluble fraction from fast pyrolysis liquids (pyrolytic lignin): part II. GPC, carbonyl groups, and <sup>13</sup>C-NMR. *J Anal Appl Pyrolysis* 58–59:387–400
  46. Kosa M, Ben H, Theliander H, Ragauskas AJ (2011) Pyrolysis oils from CO<sub>2</sub> precipitated Kraft lignin. *Green Chem* 13(11):3196
  47. Ben H, Ragauskas AJ (2011) NMR characterization of pyrolysis oils from Kraft lignin. *Energy Fuel* 25(5):2322–2332
  48. Huang Y, Wei Z, Qiu Z, Yin X, Wu C (2012) Study on structure and pyrolysis behavior of lignin derived from corncob acid hydrolysis residue. *J Anal Appl Pyrolysis* 93:153–159
  49. Ke J, Singh D, Yang X, Chen S (2011) Thermal characterization of softwood lignin modification by termite *Coptotermes formosanus* (Shiraki). *Biomass Bioenergy* 35(8):3617–3626
  50. Liu Q, Wang S, Zheng Y, Luo Z, Cen K (2008) Mechanism study of wood lignin pyrolysis by using TG–FTIR analysis. *J Anal Appl Pyrolysis* 82(1):170–177
  51. Liu Q, Zhong Z, Wang S, Luo Z (2011) Interactions of biomass components during pyrolysis: a TG-FTIR study. *J Anal Appl Pyrolysis* 90(2):213–218
  52. Shen DK, Gu S, Luo KH, Wang SR, Fang MX (2010) The pyrolytic degradation of wood-derived lignin from pulping process. *Bioresour Technol* 101(15):6136–6146
  53. Wang S, Wang K, Liu Q, Gu Y, Luo Z, Cen K, Fransson T (2009) Comparison of the pyrolysis behavior of lignins from different tree species. *Biotechnol Adv* 27(5):562–567
  54. Mullen CA, Strahan GD, Boateng AA (2009) Characterization of various fast-pyrolysis bio-oils by NMR spectroscopy. *Energy Fuel* 23(5):2707–2718
  55. Luo Z, Wang S, Guo X (2012) Selective pyrolysis of Organosolv lignin over zeolites with product analysis by TG-FTIR. *J Anal Appl Pyrolysis* 95:112–117
  56. Joseph J, Baker C, Mukkamala S, Beis SH, Wheeler MC, DeSisto WJ, Jensen BL, Frederick BG (2010) Chemical shifts and

- lifetimes for nuclear magnetic resonance (NMR) analysis of biofuels. *Energy Fuel* 24(9):5153–5162
57. Gr G, Li J, Eide I, Kleinert M, Barth T (2008) Chemical structures present in biofuel obtained from lignin. *Energy Fuel* 22(6):4240–4244
  58. DeSisto WJ, Hill N, Beis SH, Mukkamala S, Joseph J, Baker C, Ong T-H, Stemmler EA, Wheeler MC, Frederick BG, van Heiningen A (2010) Fast pyrolysis of pine sawdust in a fluidized-bed reactor. *Energy Fuel* 24(4):2642–2651
  59. David K, Kosa M, Williams A, Mayor R, Realff M, Muzzy J, Ragauskas A (2010) <sup>31</sup>P-NMR analysis of bio-oils obtained from the pyrolysis of biomass. *Biofuels* 1(6):839–845
  60. David K, Ben H, Muzzy J, Feik C, Iisa K, Ragauskas A (2012) Chemical characterization and water content determination of bio-oils obtained from various biomass species using <sup>31</sup>P NMR spectroscopy. *Biofuels* 3(2):123–128
  61. Ben H, Ragauskas AJ (2011) Pyrolysis of Kraft lignin with additives. *Energy Fuel* 25(10):4662–4668
  62. Ben H, Ragauskas AJ (2011) Heteronuclear single-quantum correlation–nuclear magnetic resonance (HSQC–NMR) fingerprint analysis of pyrolysis oils. *Energy Fuel* 25(12):5791–5801
  63. Beis SH, Mukkamala S, Hill N, Joseph J, Baker C, Jensen B, Stemmler EA, Wheeler MC, Frederick BG, van Heiningen A, Berg AG, DeSisto WJ (2010) Fast pyrolysis of lignins. *BioRes* 5(3):1408–1424
  64. Runnebaum RC, Nimmanwudipong T, Block DE, Gates BC (2012) Catalytic conversion of compounds representative of lignin-derived bio-oils: a reaction network for guaiacol, anisole, 4-methylanisole, and cyclohexanone conversion catalysed by Pt/ $\gamma$ -Al<sub>2</sub>O<sub>3</sub>. *Cat Sci Tec* 2(1):113
  65. Mortensen PM, Grunwaldt JD, Jensen PA, Knudsen KG, Jensen AD (2011) A review of catalytic upgrading of bio-oil to engine fuels. *Appl Catal, A* 407(1–2):1–19
  66. Huber GW, Iborra S, Corma A (2006) Synthesis of transportation fuels from biomass: chemistry, catalysts, and engineering. *Chem Rev* 106(9):4044–4098
  67. Czernik S, Bridgwater AV (2004) Overview of applications of biomass fast pyrolysis oil. *Energy Fuels* 18(2):590–598
  68. Wang Y, Fang Y, He T, Hu H, Wu J (2011) Hydrodeoxygenation of dibenzofuran over noble metal supported on mesoporous zeolite. *Catal Commun* 12(13):1201–1205
  69. Chantal PD, Kaliaguine S, Grandmaison JL (1985) Reactions of phenolic compounds over HZSM-5. *Appl Catal* 18(1):133–145
  70. Gayubo AG, Aguayo AT, Atutxa A, Aguado R, Bilbao J (2004) Transformation of oxygenate components of biomass pyrolysis oil on a HZSM-5 zeolite. *Alcohols and phenols*. *Ind Eng Chem Res* 43(11):2610–2618
  71. Zhu X, Mallinson RG, Resasco DE (2010) Role of transalkylation reactions in the conversion of anisole over HZSM-5. *Appl Catal A* 379(1–2):172–181
  72. Wildschut J, Iqbal M, Mahfud FH, Cabrera IM, Venderbosch RH, Heeres HJ (2010) Insights in the hydrotreatment of fast pyrolysis oil using a ruthenium on carbon catalyst. *Energy Environ Sci* 3(7):962
  73. Furimsky E (1983) Chemistry of catalytic hydrodeoxygenation. *Catal Rev-Sci Eng* 25(3):421–458
  74. Furimsky E (2000) Catalytic hydrodeoxygenation. *Appl Catal A* 199(2):147–190
  75. Elliott DC (2007) Historical developments in hydroprocessing bio-oils. *Energy Fuel* 21(3):1792–1815
  76. Choudhary TV, Phillips CB (2011) Renewable fuels via catalytic hydrodeoxygenation. *Appl Catal A* 397(1–2):1–12
  77. Bu Q, Lei H, Zacher AH, Wang L, Ren S, Liang J, Wei Y, Liu Y, Tang J, Zhang Q, Ruan R (2012) A review of catalytic hydrodeoxygenation of lignin-derived phenols from biomass pyrolysis. *Bioresour Technol* 124:470–477
  78. IEA Energy Technology Essentials (2007). Hydrogen Production and Distribution. <http://www.iea.org/techno/essentials5.pdf>. Accessed Feb 18, 2013
  79. Pan C, Chen A, Liu Z, Chen P, Lou H, Zheng X (2012) Aqueous-phase reforming of the low-boiling fraction of rice husk pyrolyzed bio-oil in the presence of platinum catalyst for hydrogen production. *Bioresour Technol* 125:335–339
  80. Wright MM, Román-Leshkov Y, Green WH (2012) Investigating the techno-economic trade-offs of hydrogen source using a response surface model of drop-in biofuel production via bio-oil upgrading. *Biofuels, Bioprod Biorefin* 6(5):503–520
  81. Wright MM, Satrio JA, Brown RC, Daugaard DE, Hsu DD (2010) Techno-economic analysis of biomass fast pyrolysis to transportation fuels. Technical Report by NREL.
  82. Jones S, Holladay J, Valkenburg C, Stevens D, Walton C, Kinchin C, Elliott D, Czernik S (2009) Production of gasoline and diesel from biomass via fast pyrolysis, hydrotreating and hydrocracking: a design case. PNNL-18284.
  83. Odebunmi EO, Ollis DF (1983) Catalytic hydrodeoxygenation: I. Conversions of o-, p-, and m-cresols. *J Catal* 80(1):56–64
  84. Odebunmi EO, Ollis DF (1983) Catalytic hydrodeoxygenation: II. Interactions between catalytic hydrodeoxygenation of m-cresol and hydrodesulfurization of benzothiophene and dibenzothiophene. *J Catal* 80(1):65–75
  85. Gevert BS, Otterstedt JE, Massoth FE (1987) Kinetics of the HDO of methyl-substituted phenols. *Appl Catal* 31(1):119–131
  86. Elliott DC, Beckman D, Bridgwater AV, Diebold JP, Gevert SB, Solantausta Y (1991) Developments in direct thermochemical liquefaction of biomass: 1983–1990. *Energy Fuel* 5(3):399–410
  87. Viljava TR, Komulainen RS, Krause AOI (2000) Effect of H<sub>2</sub>S on the stability of CoMo/Al<sub>2</sub>O<sub>3</sub> catalysts during hydrodeoxygenation. *Catal Today* 60(1–2):83–92
  88. Furimsky E, Massoth FE (1999) Deactivation of hydroprocessing catalysts. *Catal Today* 52(4):381–495
  89. Laurent E, Delmon B (1994) Influence of water in the deactivation of a sulfided NiMo $\gamma$ -Al<sub>2</sub>O<sub>3</sub> catalyst during hydrodeoxygenation. *J Catal* 146(1):281–291
  90. Centeno A, Laurent E, Delmon B (1995) Influence of the support of CoMo sulfide catalysts and of the addition of potassium and platinum on the catalytic performances for the hydrodeoxygenation of carbonyl, carboxyl, and guaiacol-type molecules. *J Catal* 154(2):288–298
  91. Honkela ML, Björk J, Persson M (2012) Computational study of the adsorption and dissociation of phenol on Pt and Rh surfaces. *PCCP* 14(16):5849
  92. Niquille-Röthlisberger A, Prins R (2006) Hydrodesulfurization of 4,6-dimethyldibenzothiophene and dibenzothiophene over alumina-supported Pt, Pd, and Pt-Pd catalysts. *J Catal* 242(1):207–216
  93. Tang T, Yin C, Wang L, Ji Y, Xiao F-S (2007) Superior performance in deep saturation of bulky aromatic pyrene over acidic mesoporous beta zeolite-supported palladium catalyst. *J Catal* 249(1):111–115
  94. Schuman S, Field S (1970) Hydrogenation of sulphite waste liquor. CA Patent 851709, 15 Sept 1970
  95. Ryymin E-M, Honkela ML, Viljava T-R, Krause AOI (2010) Competitive reactions and mechanisms in the simultaneous HDO of phenol and methyl heptanoate over sulphided NiMo/ $\gamma$ -Al<sub>2</sub>O<sub>3</sub>. *Appl Catal A* 389(1–2):114–121
  96. Lin Y-C, Li C-L, Wan H-P, Lee H-T, Liu C-F (2011) Catalytic hydrodeoxygenation of guaiacol on Rh-based and sulfided CoMo and NiMo catalysts. *Energy Fuel* 25(3):890–896
  97. Jongerijs AL, Jastrzebski R, Bruijninx PCA, Weckhuysen BM (2012) CoMo sulfide-catalyzed hydrodeoxygenation of lignin model compounds: an extended reaction network for the conversion of monomeric and dimeric substrates. *J Catal* 285(1):315–323

98. Ruinat de Brimont M, Dupont C, Daudin A, Geantet C, Raybaud P (2012) Deoxygenation mechanisms on Ni-promoted MoS<sub>2</sub> bulk catalysts: a combined experimental and theoretical study. *J Catal* 286:153–164
99. Bui VN, Laurenti D, Afanasiev P, Geantet C (2011) Hydrodeoxygenation of guaiacol with CoMo catalysts. Part I: promoting effect of cobalt on HDO selectivity and activity. *Appl Catal, B* 101(3–4):239–245
100. Romero Y, Richard F, Brunet S (2010) Hydrodeoxygenation of 2-ethylphenol as a model compound of bio-crude over sulfided Mo-based catalysts: promoting effect and reaction mechanism. *Appl Catal, B* 98(3–4):213–223
101. Badawi M, Paul JF, Cristol S, Payen E, Romero Y, Richard F, Brunet S, Lambert D, Portier X, Popov A, Kondratieva E, Goupil JM, El Fallah J, Gilson JP, Mariey L, Travert A, Maugé F (2011) Effect of water on the stability of Mo and CoMo hydrodeoxygenation catalysts: a combined experimental and DFT study. *J Catal* 282(1):155–164
102. Do PTM, Foster AJ, Chen J, Lobo RF (2012) Bimetallic effects in the hydrodeoxygenation of meta-cresol on  $\gamma$ -Al<sub>2</sub>O<sub>3</sub> supported Pt–Ni and Pt–Co catalysts. *Green Chem* 14(5):1388
103. Hong D-Y, Miller SJ, Agrawal PK, Jones CW (2010) Hydrodeoxygenation and coupling of aqueous phenolics over bifunctional zeolite-supported metal catalysts. *Chem Commun* 46(7):1038
104. Lee CR, Yoon JS, Suh Y-W, Choi J-W, Ha J-M, Suh DJ, Park Y-K (2012) Catalytic roles of metals and supports on hydrodeoxygenation of lignin monomer guaiacol. *Catal Commun* 17:54–58
105. Zhu X, Lobban LL, Mallinson RG, Resasco DE (2011) Bifunctional transalkylation and hydrodeoxygenation of anisole over a Pt/HBeta catalyst. *J Catal* 281(1):21–29
106. Pham TT, Lobban LL, Resasco DE, Mallinson RG (2009) Hydrogenation and hydrodeoxygenation of 2-methyl-2-pentenal on supported metal catalysts. *J Catal* 266(1):9–14
107. Ohta H, Kobayashi H, Hara K, Fukuoka A (2011) Hydrodeoxygenation of phenols as lignin models under acid-free conditions with carbon-supported platinum catalysts. *Chem Commun* 47(44):12209
108. Li N, Tompsett GA, Zhang T, Shi J, Wyman CE, Huber GW (2011) Renewable gasoline from aqueous phase hydrodeoxygenation of aqueous sugar solutions prepared by hydrolysis of maple wood. *Green Chem* 13(1):91
109. Gutierrez A, Kaila RK, Honkela ML, Slioor R, Krause AOI (2009) Hydrodeoxygenation of guaiacol on noble metal catalysts. *Catal Today* 147(3–4):239–246
110. Liu C, Shao Z, Xiao Z, Williams CT, Liang C (2012) Hydrodeoxygenation of benzofuran over silica–alumina-supported Pt, Pd, and Pt–Pd catalysts. *Energy Fuel* 26(7):4205–4211
111. Beccat P, Bertolini JC, Gauthier Y, Massardier J, Ruiz P (1990) Crotonaldehyde and methylcrotonaldehyde hydrogenation over Pt(111) and Pt<sub>80</sub>Fe<sub>20</sub>(111) single crystals. *J Catal* 126(2):451–456
112. Birchem T, Pradier CM, Berthier Y, Cordier G (1994) Reactivity of 3-methyl-crotonaldehyde on Pt(111). *J Catal* 146(2):503–510
113. Jiang H, Yang H, Hawkins R, Ring Z (2007) Effect of palladium on sulfur resistance in Pt–Pd bimetallic catalysts. *Catal Today* 125(3–4):282–290
114. Bonalumi N, Vargas A, Ferri D, Baiker A (2006) Theoretical and spectroscopic study of the effect of ring substitution on the adsorption of anisole on platinum. *J Phys Chem B* 110(20):9956–9965
115. Lu S, Lonergan WW, Bosco JP, Wang S, Zhu Y, Xie Y, Chen JG (2008) Low temperature hydrogenation of benzene and cyclohexene: a comparative study between  $\gamma$ -Al<sub>2</sub>O<sub>3</sub> supported PtCo and PtNi bimetallic catalysts. *J Catal* 259(2):260–268
116. Lu S, Menning CA, Zhu Y, Chen JG (2009) Correlating benzene hydrogenation activity with binding energies of hydrogen and benzene on Co-based bimetallic catalysts. *ChemPhysChem* 10(11):1763–1765
117. Lonergan WW, Vlachos DG, Chen JG (2010) Correlating extent of Pt–Ni bond formation with low-temperature hydrogenation of benzene and 1,3-butadiene over supported Pt/Ni bimetallic catalysts. *J Catal* 271(2):239–250
118. Zhao C, He J, Lemonidou AA, Li X, Lercher JA (2011) Aqueous-phase hydrodeoxygenation of bio-derived phenols to cycloalkanes. *J Catal* 280(1):8–16
119. Zhao C, Kou Y, Lemonidou AA, Li X, Lercher JA (2009) Highly selective catalytic conversion of phenolic bio-oil to alkanes. *Angew Chem Int Ed* 48(22):3987–3990
120. Zhao C, Lercher JA (2012) Selective hydrodeoxygenation of lignin-derived phenolic monomers and dimers to cycloalkanes on Pd/C and HZSM-5 catalysts. *ChemCatChem* 4(1):64–68
121. Velu S, Kapoor MP, Inagaki S, Suzuki K (2003) Vapor phase hydrogenation of phenol over palladium supported on mesoporous CeO<sub>2</sub> and ZrO<sub>2</sub>. *Appl Catal A* 245(2):317–331
122. Chen YZ, Liaw CW, Lee LI (1999) Selective hydrogenation of phenol to cyclohexanone over palladium supported on calcined Mg/Al hydrotalcite. *Appl Catal A* 177(1):1–8
123. Neri G, Visco AM, Donato A, Milone C, Malentacchi M, Gubitosa G (1994) Hydrogenation of phenol to cyclohexanone over palladium and alkali-doped palladium catalysts. *Appl Catal A* 110(1):49–59
124. Talukdar AK, Bhattacharyya KG, Sivasanker S (1993) Hydrogenation of phenol over supported platinum and palladium catalysts. *Appl Catal A* 96(2):229–239
125. Orita H, Itoh N (2004) Simulation of phenol formation from benzene with a Pd membrane reactor: a b initio periodic density functional study. *Appl Catal A* 258(1):17–23
126. Ihm H, White JM (2000) Stepwise dissociation of thermally activated phenol on Pt(111). *J Phys Chem B* 104(26):6202–6211
127. Xu X, Friend CM (1989) The role of coverage in determining adsorbate stability: phenol reactivity on rhodium(111). *J Phys Chem* 93(24):8072–8080
128. Kluson P, Cervený L (1996) Hydrogenation of substituted aromatic compounds over a ruthenium catalyst. *J Mol Catal A Chem* 108(2):107–112
129. Guo J, Ruan R, Zhang Y (2012) Hydrotreating of phenolic compounds separated from bio-oil to alcohols. *Ind Eng Chem Res* 51(19):6599–6604
130. Greenfield H (1973) Studies in nuclear hydrogenation. *Ann NY Acad Sci* 214(1):233–242
131. Nimmanwudipong T, Runnebaum R, Block D, Gates B (2011) Catalytic reactions of guaiacol: reaction network and evidence of oxygen removal in reactions with hydrogen. *Catal Lett* 141(6):779–783
132. Runnebaum R, Nimmanwudipong T, Block D, Gates B (2011) Catalytic conversion of anisole: evidence of oxygen removal in reactions with hydrogen. *Catal Lett* 141(6):817–820
133. Sato S, Takahashi R, Sodesawa T, Matsumoto K, Kamimura Y (1999) Ortho-selective alkylation of phenol with 1-propanol catalyzed by CeO<sub>2</sub>–MgO. *J Catal* 184(1):180–188
134. Auroux A, Artizzu P, Ferino I, Solinas V, Leofanti G, Padovan M, Messina G, Mansani R (1995) Dehydration of 4-methylpentan-2-ol over zirconia catalysts. *J Chem Soc Faraday Trans* 91(18):3263–3267
135. Mahata N, Raghavan KV, Vishwanathan V, Park C, Keane MA (2001) Phenol hydrogenation over palladium supported on magnesia: relationship between catalyst structure and performance. *PCCP* 3(13):2712–2719

136. Shin E-J, Keane MA (2000) Gas-phase hydrogenation/hydrogenolysis of phenol over supported nickel catalysts. *Ind Eng Chem Res* 39(4):883–892
137. Aprile C, Abad A, Garcia H, Corma A (2005) Synthesis and catalytic activity of periodic mesoporous materials incorporating gold nanoparticles. *J Mater Chem* 15(41):4408–4413
138. Fournier RO, Rowe JJ (1977) The solubility of amorphous silica in water at high temperatures and high pressures. *Am Mineral* 62:1052–1056
139. Lefèvre G, Duc M, Lepeut P, Caplain R, Fédoroff M (2002) Hydration of  $\gamma$ -alumina in water and its effects on surface reactivity. *Langmuir* 18(20):7530–7537
140. Britt PF, Buchanan AC, Cooney MJ, Martineau DR (2000) Flash vacuum pyrolysis of methoxy-substituted lignin model compounds. *J Org Chem* 65(5):1376–1389
141. Britt PF, Buchanan AC, Malcolm EA (2000) Impact of restricted mass transport on pyrolysis pathways for aryl ether containing lignin model compounds. *Energy Fuel* 14(6):1314–1322
142. Britt PF, Kidder MK, Buchanan AC (2007) Oxygen substituent effects in the pyrolysis of phenethyl phenyl ethers. *Energy Fuel* 21(6):3102–3108
143. Kawamoto H, Nakamura T, Saka S (2008) Pyrolytic cleavage mechanisms of lignin–ether linkages: a study on p-substituted dimers and trimers. *Holzforschung* 62:50–56
144. Kawamoto H, Ryoritani M, Saka S (2008) Different pyrolytic cleavage mechanisms of  $\beta$ -ether bond depending on the side-chain structure of lignin dimers. *J Anal Appl Pyrolysis* 81(1):88–94
145. Kawamoto H, Saka S (2007) Role of side-chain hydroxyl groups in pyrolytic reaction of phenolic  $\beta$ -ether type of lignin dimer. *J Wood Chem Technol* 27(2):113–120
146. Kawamoto H, Horigoshi S, Saka S (2007) Pyrolysis reactions of various lignin model dimers. *J Wood Sci* 53(2):168–174
147. Beis SH, Mukkamala S, Hill N, Joseph J, Baker C, Jensen B, Stemmler EA, Wheeler MC, Frederick BG, Av H, Berg AG, DeSisto WJ (2010) Fast pyrolysis of lignins. *BioRes* 5:17